Starch nanoparticles: modifications, toxicity, and drug loading

by

Ziyi Sun

A thesis

presented to the University of Waterloo

in fulfillment of the

thesis requirement for the degree of

Master of Science

in

Chemistry

Waterloo, Ontario, Canada, 2015

Author's Declaration

I hereby declare that I am the sole author of this thesis. This is a true copy of the thesis, including any required final revisions, as accepted by my examiners. I understand that my thesis may be made electronically available to the public.

Abstract

Nanoparticles as drug delivery vehicles have been well tested and transferred into clinical practice in the past few decades. The success of most nanocarriers is attributed to their biocompatibility, controlled release and unique size-dependent properties. In this regard, I proposed that starch nanoparticles (SNPs) might be a good candidate for drug delivery due to their excellent biocompatibility. The crosslinked SNPs supplied by EcoSynthetix Inc. are nanogel-like materials with many potential advantages, including good biocompatibility, biodegradability, and high capacity for loading drugs. In addition, SNPs can be engineered to achieve targeted delivery and sustained release of drugs. So far the SNPs from EcoSynthetix are only used commercially in the paper coating industry. The chemical modifications of SNPs are expected to generate new materials that can be used for drug and gene delivery. Since the safety of nanomaterial is of great concern in biomedical applications, one objective of this research is to study the toxicity of the unmodified and modified SNPs. Through my research, the reason for the toxicity is attributed to free crosslinker molecules present in the sample, and they can be removed by washing. For drug loading study, doxorubicin (Dox), a highly effective clinical anticancer drug, was chosen as the model drug. Due to the significant side effects of Dox, it is important to develop targeted delivery vehicles to decrease its toxicity to the healthy tissues. While several biocompatible nanocarriers have been developed to deliver Dox, the synthesis of these vehicles is often complicated and expensive. Compared to these delivery platforms, the SNPs are renewable and can be produced commercially on a large scale. Therefore, the second objective is to synthesize and characterize carboxyl-modified SNPs for Dox loading. The drug loading/release kinetics and the efficacy of drug complex were studied and compared to that of the free drug. Finally, cationic SNPs developed by a co-worker were evaluated and utilized for DNA delivery. DNA adsorption onto the cationic SNPs was investigated, and then the cellular uptake efficiency of the DNA/SNPs complexes was were tested and formed to be comparable to a commercial gene transfection agent. This new generation of SNP platform holds great promise for the treatment of cancer in the future.

Acknowledgements

I would like to express my great gratitude and appreciation to my supervisor, Dr. Juewen Liu for all his consistent guidance, support and encouragement. His valuable guidance and advice helped me overcome the difficulty and discover new aspects in my research.

I would also like to extend thanks to the members of my committee, Dr. Jean Duhamel, and Dr. Michael Tam for their time to read my thesis and their valuable suggestions.

I really enjoyed working with my colleagues in Dr. Liu's group in the last two years. They are smart, diligent and eager to help with every aspect of the project. I am so thankful to receive the professional trainings from Dr. Feng Wang and Jimmy Huang during my project. I learned valuable experimental skills, especially in cell experiments and gel electrophoresis. I want to give special thanks to Biwu Liu for his assistance with equipment, discussion of ideas, patience and encouragement when I lost direction. I also want to thank all other group members for their help and support.

I would also like to acknowledge EcoSynthetix Inc., all the ECO-WIN group members and Eco-WIN professors Dr. Jean Duhamel, Dr. Scott Taylor, and Dr. Mario Gauthier for their tireless discussion and valuable suggestions in the project progress meetings.

Lastly, I would like to thank my parents and friends for their endless support and encouragement.

Table of Contents

Table of Figures

List of Abbreviations

AuNP: gold nanoparticle

CHPTMA: 3-chloro-2-hydroxypropyltrialkylammonium chlorides

Cisplatin/cisPt: cis-dichlorodiamine platinum(II)

DLS: dynamic light scattering

DMEM: Dulbecco's modified eagle medium

DMSO: dimethyl sulfoxide

DNA: deoxyribonucleic acid

DOTAP: 1,2-dioleoyl-3-trimethylammonium-propane (chloride salt)

Dox: doxorubicin · hydrochloride

FAM: 6-carboxyfluorescein

FBS: fetal bovine serum

FDA: US Food and Drug Administration

GX: glyoxal

HEPES: 4-(2-hydroxyethyl)-1-piperazineethanesulfonic acid

MTT: 3-(4,5-Dimethylthiazol-2-yl)-2,5-diphenyltetrazolium bromide

PBS: phosphate buffered saline

PEG: poly (ethylene glycol)

PEI: polyethylenimine

PLGA: poly (lactic-co-glycolic) acid

SNP-COOH: oxidized starch nanoparticles

SNPs: starch nanoparticles

TBE: tris-borate-EDTA buffer

TEMPO: 2,2,6,6-tetramethylpiperidine-1-oxyl

UV-vis: Ultraviolet-visible spectroscopy

Chapter 1 Introduction

1.1 Cancer and cancer therapy

Cancer refers to out-of-control cell growth that can invade normal tissues. Many people around the world are suffering from more than 100 types of cancers.[1] Based on the report from the American Cancer Society, cancer is the second largest cause of death in the US and 589,430 Americans are expected to die due to cancer in 2015.[2] Current cancer treatments include surgery, radiation therapy, chemotherapy and other methods. Each treatment has pros and cons depending on the cancer types, location and patient status. Surgery and radiotherapy are highly targeted treatments to remove the entire malignant tumor. However, once the cancer has spread throughout the body via metastases, these methods have limited impact. Moreover, surgery and radiotherapy require good patient conditions due to their high invasiveness.[3]

Chemotherapy is another treatment commonly used to control the growth of tumors by drug administration. These drugs can suppress tumor cell replication via targeting cell mitosis.[3] However, chemotherapeutic drugs kill not only cancerous cells, but also healthy cells. The effectiveness of chemotherapy is limited by their toxic side effects, including hair loss, weight loss, vomit, skin sensitization, and immunosuppression. Another major limitation to effective chemotherapy is drug resistance.[4] The amount of drug reaching target cells is insufficient to kill cancer cells, therefore dosage must be increased. However, a high dosage also enhances the risk of toxic side effects to normal tissues.[4] Therefore, it is urgent to develop targeted chemotherapy to cancer cells and decrease side effects to normal tissues.

1.2 Advantages of nanomaterials as drug carriers

As the emerging nanotechnology is moving at a fast pace, the application of nanotechnology in biomedicine has attracted intense research interest in recent years.[5]

Nanotechnology involves nanomaterials with at least one dimension having a size between 1 to 100 nanometers. Compared to free drugs, nanoscale vehicles can offer many advantages, such as enhanced drug solubility, protection from unspecific interaction, longer circulation time, improved targeting efficiency, and controlled release at specific sites.[5] The cell uptake of nanocarriers is greatly affected by the physicochemical properties of nanoparticles, drugs, and environmental parameters.[5] A systemic understanding of such effects is vital for the successful design and development of drug delivery vehicles. In this section, some key properties of nanomaterials affecting drug delivery are discussed.

1.2.1 Size of nanomaterials

It is generally accepted that nanoparticles with a diameter of 10-100 nm are suitable for cell uptake.[6] Smaller particles (< 5 nm) are easily cleared by glomerular filtration in the kidneys, while particles larger than 100 nm have low permeation into tumor cells. Researches show that 40-50 nm of nanoparticles have the highest uptake efficieny.[7] It is considered that the internalization mechanisms of particles with various sizes may be different. When particles are larger than 1 μm, they are internalized mainly through the phagocytosis mechanism. Smaller nanoscaled particles enter cells through the pinocytosis mechanism via unspecific and/or specific interaction with cell membrane followed by internalization.[7] Therefore, the size range of nanomaterials allows it to possess a longer biological half-life compared to small molecular cancer drugs.

1.2.2 Surface properties of nanoparticles

The loading capacity of various drugs can be achieved through covalent bonding, hydrophobic interaction, electrostatic interaction, etc.[5] Many hydrophobic drugs have low solubility. To achieve high-performance therapy, a high concentration of drugs is always

required. Therefore, it is beneficial to improve the solubility of drugs using nanocarriers. Ideally nanocarriers can prevent unspecific interactions with the biological environment, and protect drugs from unnecessary degradation. Additionally, multiple types of drugs with different functionalities can be co-delivered using the high surface area of nanomaterials. Drug release inside the cell can be controlled by environmental stimuli if responsive functional groups are attached to the surface of nanomaterials.

Surface charge is another important factor affecting the internalization of nanoparticles. Positively charged particles may interact electrostatically with the cell membranes containing negatively charged phospholipid head groups, which facilitates the cellular binding and uptake. The internalization pathway could be controlled by endocytic modes due to the creation of holes in the membrane. Macropinocytosis could be an important mechanism for positively charged particles.[8] Particles with negative charges may interact with cell membrane proteins. The internalization was suggested to be a dymamin-independent manner. More studies are required to investigate the exact pathway for the internalization of the nanoparticles with various charges. Non-specific interactions of nanoparticles (either negative or positive) with proteins or other components in serum may induce elevated clearance.

1.2.3 Passive and active targeting

Nanocarriers offer a unique high efficiency of drug delivery into the tumor cells via either passive or active pathways. The passive pathway can be explained by the enhanced permeation retention (EPR) effect shown in Figure 1. Typically, tumor cells have leaky blood vessels. To maintain rapid cell growth, tumor tissues show high vascular permeability, allowing more nutrients and oxygen into the tumor cell. Macromolecules with molecular weight (MW) larger than 40 kDa prefer to accumulate in the tumor tissues. As a result, retained nanocarriers with a

similar size can concentrate and then release drugs into the tumor cells. Although passive targeting is a popular strategy, limitations still exist. For example, certain tumors or some part of tumors do not exhibit the EPR effect. One promising strategy to overcome the limitations is to use active targeting.

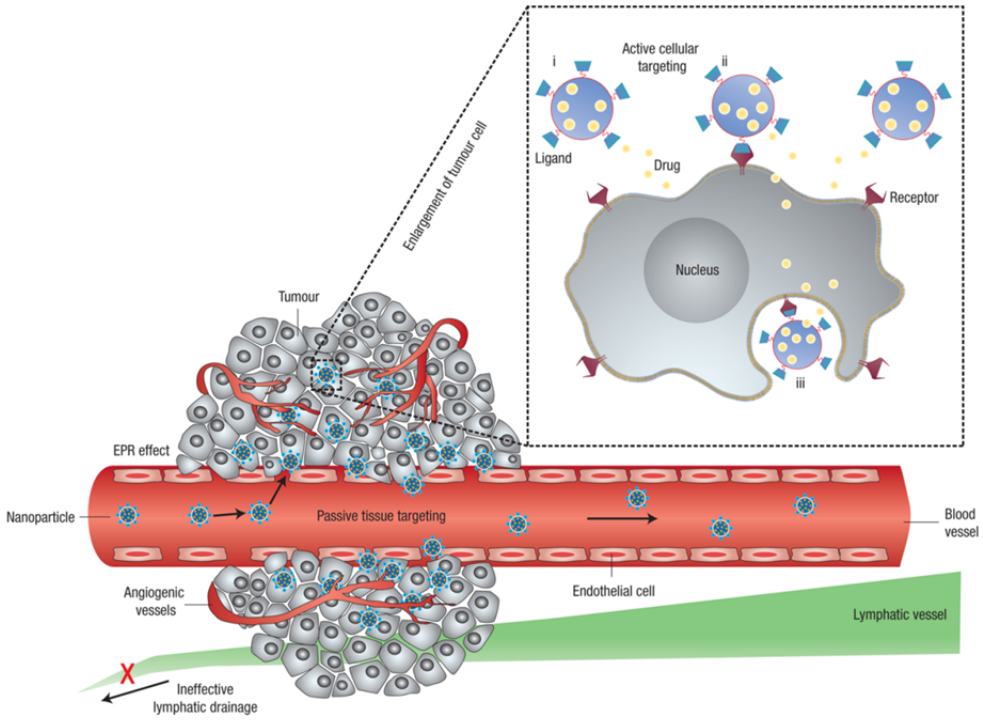

Figure 1. Targeted delivery of nanocarriers into the tumor cells via two mechanisms: passive targeting (EPR effect) and active targeting (receptor targeting). This figure is adapted from ref. [5] Copyright 2007, Nature Publishing Group.

Active targeting involves the functionalization of nanocarriers with targeting chemical ligands. These nanocarriers with targeting ligands can recognise specific groups called receptors on the cell surface. After targeting cancer cells with receptors at the surface (shown in Figure 1), the nanocarriers will be internalized into the tumor cells, followed by the drug release. The specific binding to cell surface receptors facilitates the accumulation of drugs into cancer cells.

Compared to free drugs and passive targeting, active targeting can increase the possibility of tumor cell uptake, improve therapeutic effects and decrease side effect to normal cells. Selecting the suitable targeting receptors plays a vital role in the successful design of an active targeting nanocarrier. Receptors overexpressed on the cancer cell surface are preferred, such as human epidermal growth factor receptor 2 (HER2) in breast cancers, the folate receptor in ovarian cancer, luteinizing-hormone-releasing hormone (LHRH) receptor in many cancers. Targeting ligands can be screened based on the receptor of tumor cells. Aptamers, proteins, antibodies and their fragments are the most widely used ligands.[9] Peptides also have been used as targeting ligands due to their easy preparation, low cost, and enhanced resistance to enzymatic degradation.[9]

1.2.4 Biocompatibility and biodegradability

Many types of nanomaterials have been developed as drug delivery vehicles over the past few decades. Although each type of drug-carriers has its unique advantages and drawbacks, their safety as carriers in drug delivery systems causes great concern. Some inorganic nanomaterials possess optical and magnetic properties, but it is hard to ignore their inflammatory effect and toxicity on cells after repeated administration.[10] For examples, studies have shown that nanoparticles of titanium oxide can induce DNA damage and cell death.[11] Carbon nanotubes, as emerging drug delivery platforms, have been reported to cause granulomas in lungs of laboratory animals.[12–14] As a result, research has focused on developing more biocompatible nanoparticles, such as liposomes and biocompatible polymeric nanoparticles. To avoid the unspecific interactions with plasma proteins, the surface of nanoparticles is typically modified with non-charged hydrophilic PEG chains via PEGylation. Several studies have shown that PEGylated

nanoparticles have longer circulation time *in vivo*.[15,16] Optimization of PEG molecular weight and layer thickness is required to achieve the best efficacy.

1.3 Nanomaterials as drug delivery vehicles

Over the past few decades, many types of nanomaterials have been developed as drug delivery vehicles. Besides their unique size and surface properties, each nanomaterial offers additional functionalities to improve the pharmacokinetics and pharmacodynamics of cancer drugs. Herein, three widely investigated nanocarriers (liposomes, polymeric nanomaterials, and inorganic nanoparticles) are introduced. The properties, applications and development of these nanocarrier platforms are introduced in the following sections.

1.3.1 Liposome-based drug delivery

Liposomes, spherical vesicles of lipid bilayers, have attracted strong interest for biomedical applications. The physicochemical properties of liposomes are determined by the hydrophilic headgroups, linkers and hydrophobic tails. For example, the thickness of the bilayer and the phase transition temperature (T_m) of liposomes depend on the length of the carbon chain. The charge and type of headgroups control the interaction modes of liposomes with proxy molecules. Incorporation of synthetic lipids into naturally occurring liposomes provides rich possibilities for biomedical applications.[17]

Liposomes as drug delivery vehicles represent the first generation of nanoparticle drug delivery platforms and are still the most successful systems. Due to their amphiphilic structures, liposomes can carry both hydrophobic and hydrophilic drugs. Several liposome-based therapeutics (e.g. Doxil, AmBisome, and DepoCyt) have been approved by FDA.[17] In 1995, Doxil (doxorubicin•HCl liposome injection, Janssen Biotech, Inc) was approved to treat AIDS related Kaposi's syndrome.[18] Compared to the free drug Dox, Doxil offers a ~100-times longer

half-life and a reduction in cardiotoxicity. However, Doxil also shows some unwanted adverse effect, such as skin toxicity, which has not been observed for free Dox. These early approved liposomal drugs typically only contain original liposomes and delivered drugs (Figure 2A). While the simple system achieves great success, the drawbacks are obvious. For example, liposomes may eliminate entrapped drugs before the EPR effect could induce cell targeting due to their instability. To improve the targeting efficiency, ligands with recognition capability are attached to the surface of liposomes (Figure 2B). These active targeting ligands include proteins, aptamers, peptides antibodies and their fragments. Incorporating antibodies or antibody fragments into liposomes are the most common strategy for active targeting due to their high affinity toward receptors. Even with improved targeting efficiency, the unwanted leakage of drugs may still occur due to the unspecific interaction of liposomes with plasma proteins. One popular strategy is to modify the liposome surface with PEG chains (Figure 2C). The "stealth" PEG coatings also increase the circulation time. PEGylated liposome vincristine shows a 66-fold decrease in clearance compared to the free drug vincristine.[15] Furthermore, if a cleavable linker (e.g., S-S bond) is used, detachable PEG coating can be realized.[19] A simple combination of targeting ligands and surface blocking can result in novel nanocarriers with combined performance (Figure 2D). Now versatile conjugation strategies provide liposome more functionality for enhanced targeting (Figure 2E). For example, combination of liposome with magnetic nanoparticles provides magnetic resonance molecular imaging in cancer therapy.

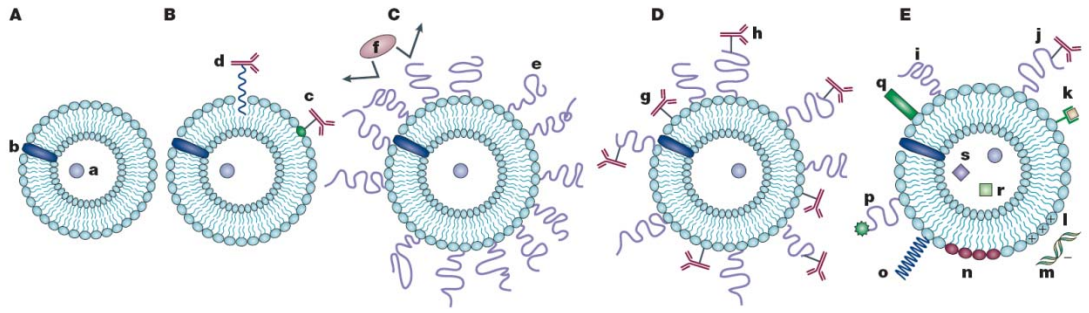

Figure 2. Development of liposome platforms as drug carriers in different stages. (A) Unmodified liposome can deliver both (a) hydrophilic drugs and (b) hydrophobic drugs. (B) Antibody as targeting compound can be (c) covalently attached or (d) incorporated into the membrane. (C) (f) A protective layer is formed by (e) PEG modification. (D) PEG layer and antibody (g, h) are combined to modify the liposome. (E) More surface functionalization strategies, including (i) protective polymer layer, (j) antibody attached polymer layer, (k) diagnostic labelling, incorporation of (l) positive charged lipids for (m) DNA adsorption, (n) responsive liposome or (o) polymer, (p) cell-penetrating peptide, (q) viral component, and (r) functional magnetic particles or (s) noble metal nanoparticles. This figure is adapted from ref. [20] Copyright 2005, Nature Publishing Group.

Although liposome-based drug delivery platforms exhibit promising results in both lab and clinic, challenges still exist, especially for active targeting. For example, the diffusion and internalization may be inhibited by the presence of targeting molecules. Also, unspecific interactions with serum proteins may deactivate the active targeting. Therefore, subsequent works are required to examine various environmental factors in the clinical applications.

1.3.2 Polymer-based drug delivery

Polymers are another widely studied drug delivery platform for cancer therapy. Both natural polymers (dextran, hyaluronic acid, chitosan) and synthetic polymers (PEG, poly(vinylpyrrolidone) (PVP)) have shown great possibilities as drug delivery systems.[21] Additionally, diverse structures of polymers (e.g. linear polymers, branched polymers, graft polymers, dendrimers) provide advantages for rational carrier design. The terminology “polymer therapeutics” was coined to describe five types of polymer-based drugs, including polymeric

drug, conjugates of polymers with proteins, complexes formed between DNA and polymers, conjugates of polymers with small molecular drugs, and block copolymer micelles loaded with drugs (Figure 3).[21]

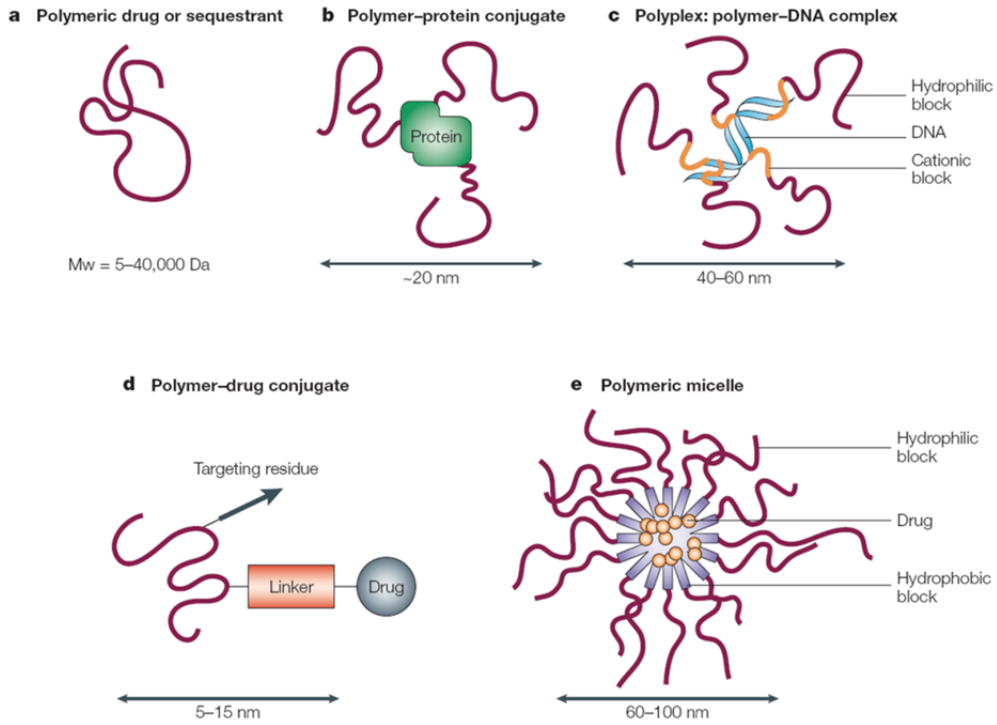

Figure 3. Scheme of representative polymer-based drug delivery platforms. This figure is adapted from ref. [21] Copyright 2003, Nature Publishing Group.

1.3.2.1 Polymeric drugs

Certain natural polymers possess intrinsic antitumor activity. For example, divinyl ether and maleic anhydride copolymer (DIVEMA) have been shown to exhibit antitumor, antibacterial, and antifungal activities.[21] However, DIVEMA failed in clinical trials due to its high toxicity. Researchers turn their attention toward modifying natural polymeric drugs to decrease toxicity. Sulfated dextrin[22] shows anti-HIV type 1 activity by blocking T-cell lines infection. Besides natural polymers, synthetic counterparts also attracted a lot of attention. Glatiramer acetate (COPAXONE, Teva Pharmaceuticals) is a synthetic polypeptide composed of four amino acids:

$_L$-ananine, $_L$-lysine, $_L$-glutamic acid and $_L$-tyrosine. With a myelin basic protein mimic property, COPAXONE is approved by FDA for reducing the frequency of relapses.[23] While polymeric drugs have intrinsic biological activities, most polymers used in drug delivery systems should be non-toxic.

1.3.2.2 Polymer-drug conjugates

Cancer drugs can be small molecules, proteins, antibodies and DNA dependent on the action mechanism. In a biological environment, these drugs suffer from poor stability and inefficient cell targeting. For example, to improve the stability of protein-based drugs, PEG was conjugated to protein drugs in the 1970s.[24] The incorporation of a PEG chain also provides proteins with several advantages: increased solubility, reduced immunogenicity, and prolonged plasma half-life. Due to these excellent advantages, several PEG-protein drugs have been approved and have reached the market.[25] Additionally, combining polymer with small molecule drugs can improve the targeting efficiency. Typically, a responsive linker group is used to link the polymer chain with the drug. As a result, unnecessary degradation can be avoided during the transport process. After accumulating on the targeting cell, the linker group is cleaved and the drug is released. Some popular strategies include enzyme-cleavable linkers and pH-sensitive linkages.

1.3.2.3 Polymeric micelles

Block copolymers can form micellar structures via self-assembly. Hydrophobic cancer drugs can be simply encapsulated into the core of the micelle. One polymeric micelle-based nanocarrier, Genexo-PM, has been approved in Korea in 2007 and has entered phase II clinical stage in the USA.[26,27] The entrapping method is simple for formulation. However, the disadvantages are obvious. The drug loading efficiencies may be affected by many

environmental factors such as solvent, temperature, hydrophobicity of polymer chain, and property of drugs. Additionally, combination of drug conjugation and entrapping into the core of micelle can achieve multi-drugs delivery. Kolishetti and co-workers reported the conjugation of Pt(IV) pro-drug into the poly(lactic acid) (PLA) chain, and entrapped doxetaxel into the core of polymeric micelles formed with PLGA-PEG-COOH using the nano-precipitation method (Figure 4).[16] Their work demonstrated that the co-delivery of drugs with different physicochemical properties could be achieved by self-assembled polymeric micelles.[16]

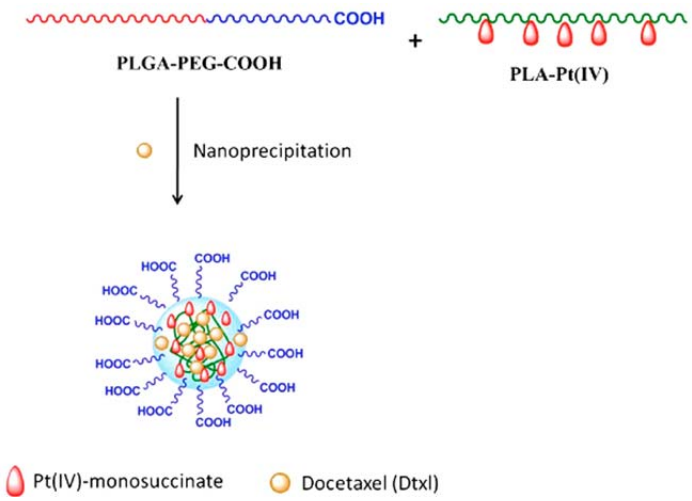

Figure 4. Co-delivery of Pt(IV) pro-drug and docetaxel by self-assembled polymeric micelles. This figure is adapted from ref. [16] Copyright 2010, The National Academy of Sciences.

1.3.3 Inorganic nanomaterials

Liposome- and polymer-based nanomaterials represent the most successful nanocarriers for cancer drugs until now. However, many potent drugs have limited abilities to be loaded into liposomes or polymer nanocarriers and need more suitable platforms. Inorganic nanoparticles have unique size dependent optical, electric, and magnetic properties. Therefore, using inorganic nanoparticles for drug delivery can provide additional functionalities, such as magnetic

resonance imaging and remote controlled release. Also, the surface of inorganic nanoparticles can be easily functionalized via many conjugating strategies to provide multiple functionalities.

1.3.3.1 Gold Nanoparticles (AuNPs)

One of the major issues faced by chemotherapy is the low solubility of hydrophobic drugs. Paclitaxel, a mitotic inhibitor, has shown great impact in cancer treatments; however, its anticancer efficacy is limited due to its low aqueous solubility. Although many lipid- and polymer-based nanocarriers successfully improved the solubility, these encapsulation methods gave a relatively large particle size. Zhang and co-workers[28] prepared a drug-nanoparticle hybrid by covalently linking Paclitaxel onto the surface of DNA modified gold nanoparticles. As shown in Figure 4, the DNA linker was labeled with two functional linking groups, a thiol and amine group, and a fluorescent dye. The DNA was conjugated with drugs (modified Paclitaxel) through EDC/Sulfo-NHS coupling chemistry; meanwhile, DNA was conjugated with AuNPs through the well-established thiol-gold chemistry. Three common problems related to Paclitaxel could be solved with this platform: 1) the solubility of Paclitaxel was enhanced in both buffers and cell culture environments. 2) The drug efficacy was increased. 3) Combined with the potent optical property of AuNPs, the movement of nanocarriers can be monitored. Besides DNA, other linkers, such as hexaethylene glycol, have also been reported to covalently attach Paclitaxel to AuNPs.[29]

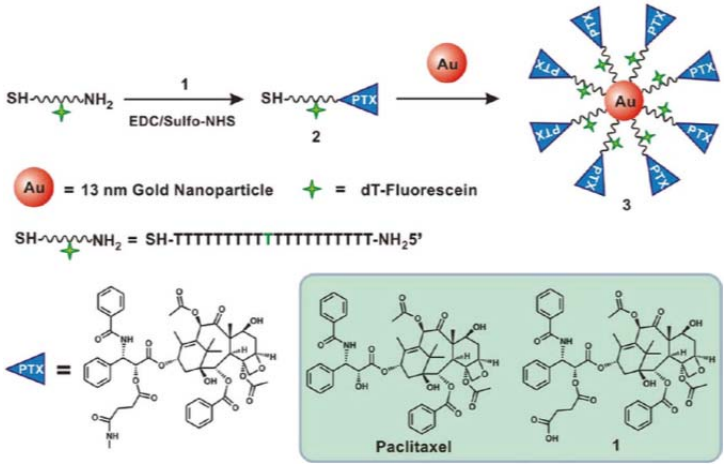

Figure 4. Schematic representation of conjugation Paclitaxel with AuNPs via a DNA linker. This figure is adapted from ref. [28] Copyright 2011, American Chemical Society.

1.3.3.2 Magnetic Nanoparticles (MNPs)

MNPs are promising drug carriers due to their unique magnetic field responsiveness. Upon application of an external magnetic field, MNPs can accumulate at specific sites until the release of contained drugs. Additionally, hyperthermia can be achieved under an external alternative magnetic field (AMF). Initially, micro-sized magnetic particles were used to deliver various drugs. For example, Widder and co-workers[30] used magnetic albumin microspheres to deliver Dox with 100-fold higher dose than for the free drug. However, the microsize of magnetic particles limits their surface area and drug loading capacity. Lübbe and co-workers[31,32] pioneered the work using nanosized magnetic particles as drug delivery vectors later on.

To obtain a high drug loading capacity, the MNPs are typically modified with an organic or inorganic shell. The core structure of the composites maintains the magnetics properties, and the shell captures and releases drugs. For example, Gang and co-workers[33] synthesized a poly(ε-caprolactone) (PCL) modified Fe_3O_4 NPs to load anticancer drug gemcitabine in the polymer

shell. A significant antitumor activity was observed at a dose 15-fold lower than for the free drugs. It is considered that attaching PEG on the particle surface could further enhance the delivery efficacy. The PEG molecules can minimize the reticuloendothelial system (RES) uptake and systemic clearance of nanoparticles. Yu and co-workers reported a cross-linked (trimethoxysilyl)propyl methacrylate-γ-PEG methacrylate-coated superparamagnetic iron oxide nanoparticles and used this conjugate to deliver Dox (Figure 5).[34] The drug Dox with positive charge was adsorbed by the carboxylic groups on the particles surface via electrostatic attraction. A significant antitumor activity at low dose (8-fold lower than the free drug) was achieved even without an external magnetic field due to the EPR effect. The magnetic core of the composite used in this work offers the capability of magnetic resonance imaging instead of therapeutic benefits.

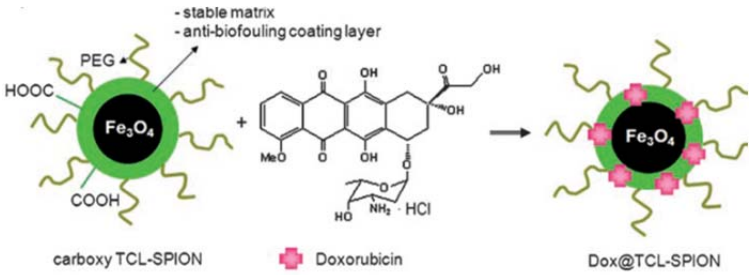

Figure 5. Scheme of formation of supermagnetic iron oxide nanoparticles for Dox loading. This figure is adapted from ref. [34] Copyright 2008, Wiley-VCH Verlag GmbH & Co. KGaA, Weinheim.

While AuNPs, magnetic NPs and other inorganic NPs have been developed as drug delivery carriers, limitations of these platforms still exist. For example, the strength of the external field applied to magnetic NPs at specific sites may be limited, due to the gradual

decrease of the magnetic field. Another issue is the unknown toxicity of the inorganic nanoparticles and their degradation products to humans.

1.4 Nanomaterials as gene delivery vehicles

Gene therapy is using functional nucleic acids as drugs to treat genetic disorders.[35] To achieve gene regulation therapy, a key issue is the development of useful gene delivery vehicles because free DNA or RNA is rapidly degraded in the blood. Until now two categories of vehicles have been involved in gene delivery: viral and nonviral vectors. The early works focused on viral vectors,[35] such as adenoviral vectors and retroviral vectors. While efficient gene transfer was obtained using viral vectors, high concern on the safety have limited their development.[36] Nonviral vector systems have attracted a large amount of research interest in the past decade. The advantages of nonviral vectors include excellent biocompatibility and their easy scale up for manufacturing. Most of current works are focusing on engineering nanomaterials with high gene transfer efficiency and stability *in vivo*. Typical nonviral vectors are cationic liposomes and cationic polymers.[37]

As early as 1979, the delivery of DNA into cells using cationic lipids was demonstrated.[38] Typically, cationic liposome, for example, 1,2-dioleoyl-3-trimethylammoniumpropane (DOTAP) and *N*-[1-(2,3-dioleyloxy)propyl-]-*N*,*N*,*N*-trimethylammonium chloride (DOTMA), are used to bind to negatively charged DNA mainly through electrostatic interaction. Researchers have found that the cationic head groups, the hydrocarbon tails, and the linking groups affect the gene delivery efficiency.[36] Since DNA can be condensed through electrostatic interaction, a straightforward strategy to improve transfection efficiency is to increase the charge density of the polar head groups. For example, the liposomes formed with dioctadecylamidoglycylspermin (DOGS), a lipid with multiple headgroups, exhibit elevated DNA delivery capability.[39] Also,

replacing the ammonium groups with phosphonium or arsonium[40] can significantly decrease the cytotoxicity and increase transfection efficiency. While head groups are directly related to DNA binding, the hydrophobic tails also affect the delivery performance. Studies indicate that the liposomes with lipids having a shorter carbon chain show higher transfer efficiency (e.g. C_{14} > C_{16} >C_{18}).[41] The cytotoxicity of liposome vectors is considered to be from the cationic headgroups.[37]

Cationic polymers also have been used as gene delivery vectors for a long time. Polyethylenimine (PEI), well known as the gold standard for gene delivery, is the most famous cationic polymer for gene delivery. Since Behr's initial work in 1995,[42] PEI and its various derivations have been proved to be effective gene transfer vectors. Jones and co-workers[37] have summarized that five important parameters need to be considered when designing a polymeric gene delivery system, including the charge density, binding site, functional group, molecular weight, and stability.[37] Nitrogen containing groups of cationic polymers are typically used as the DNA binding sites. The DNA binding capability of cationic groups on polymers follows the order: quaternary > tertiary > secondary > primary[43]; but it is interesting to note that tertiary amines rather than quaternary amines is claimed to achieve the highest gene delivery efficiency.[44] The cytotoxicity of polymer-based vectors is dependent on the chemical structure of the polymer backbone. Chemical bonds that readily hydrolyze in physiological conditions are preferred to esters, phosphoesters, and amides.

Besides these two classical gene delivery vectors, novel vectors based on quantum dots,[45] metal nanoparticles,[46] and carbon nanotubes[47] have been reported to possess high transfer efficiency as well. However, the major drawback of these inorganic nano-vectors is their unknown cytotoxicity.

1.5 Starch and starch nanoparticles

Although many drug and gene delivery vehicles have been developed in the laboratory, only limited platforms have the potential to be commercialized. Safety issues still exclude most new nano-vehicles. The success of most nanoparticle drug delivery platforms is attributed to their biocompatibility. In this regard, the use of natural products with excellent biocompatibility is still the best choice, even though some physicochemical properties may be sacrificed. Therefore, biocompatible materials such as starch are considered as being good candidates for drug delivery vehicles. However, two aspects limit the development of starch as drug vehicles. 1) the size of native starch grain is too large (micrometer scale) and is not well-defined. 2) The drug loading capacity might be low due to the limited surface area and functional groups of unmodified starch. To transform starch into useful drug delivery vehicle, preparation of nanoscaled starch particles and surface modification become prerequisites.

1.5.1 Structure and property of starch

Starch is an environment-friendly, biodegradable and biocompatible polymer produced by many plants, such as potato, corn, rice, and wheat.[48] As the major dietary source of carbohydrates, starch is the second most abundant biomaterial in nature. Besides food, starch can be used industrially to replace traditional materials due to its renewable and cost-effective advantages. To date, starch has already been investigated and used as a coating agent, thickener, adhesives, biodegradable filler in cosmetics and pharmaceuticals.[49]

The main constituent of starch is glucose. Starch consists of two polysaccharides: amylose and amylopectin. Amylose is a linear polymer, in which glucose units are linked together via α-1,4 glycosidic bonds. Amylopectin is a larger branched polymer, in which glucose units are linked together via both α-1,4 and α-1,6 glycosidic bonds.[48,50] Figure 6 illustrates the

structures of amylose and amylopectin. The size of amylopectin is much larger than that of amylose. Amylose has a molecular weight in the range of 10^5 to 10^6 g/mol, while amylopectin has a molecular weight in the range of 10^6-10^7 g/mol. Starch consists of 15-20 wt% amylose and 80-85 wt% amylopectin.[50] Starch particles are stored in plants in the form of granules. The size of a starch granule depends on the species of the plant and ranges from 1 to 200 μm.[51]

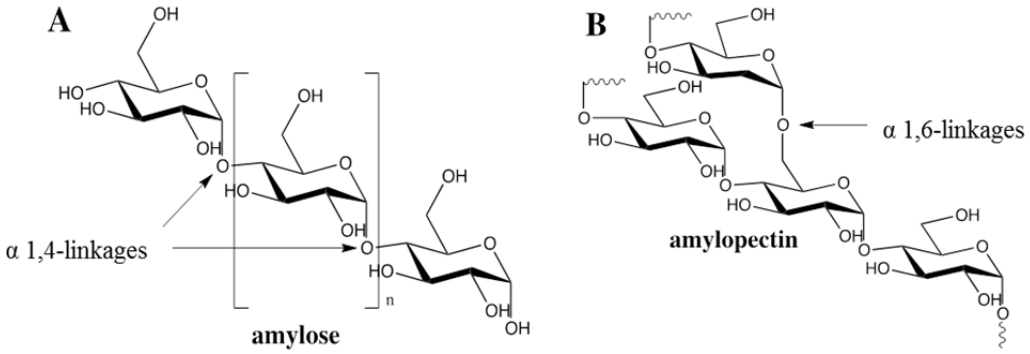

Figure 6. Molecular structures of glucose-based polysaccharides. A) Amylose with α-1,4 glycoside bonds. B) Amylopectin with both α-1,4 and α-1,6 glycoside bonds.[50]

Due to its polymeric structure and large particle size, native starch is hardly soluble in cold water. Although starch can be dispersed in water by gelatinization at high temperature, it becomes insoluble again upon reducing temperature.[49] Starch has high viscosity once it gels. The poor solubility and high viscosity of starch make it difficult to modify and this limits its potential industrial applications. However, modifications can improve the physical properties of starch and add more functional groups to starch. After modification, starch can replace more traditional materials in various fields. As a result, different techniques have been studied to reduce the size and improve the solubility of starch.

1.5.2 Starch Nanoparticles (SNPs)

1.5.2.1 Preparation of SNPs

In most recent studies, the conventional preparation process of SNPs is performed by chemically crosslinking starch molecules with appropriate crosslinking agents. Starch molecules are obtained by degradation of granular starch. Enzymes, acids and bases are commonly utilized to open the structure of natural starch.[52] Many crosslinking agents have been investigated to improve the properties of natural starch for different applications, including glyoxal,[53] phosphorus oxychloride[54], sodium tripolyphosphate,[55–58] sodium trimetaphosphate,[52] diepoxybutanes,[59] epichlorohydrin,[60–62] citric acid,[63,64] dicarboxylic acids,[65] anhydrides,[66] and dialdehydes[67]. Those agents typically have at least two binding sites, which can crosslink starch together by forming ester or ether bonds. The available crosslinking sites of starch are their abundant hydroxyl groups. Figure 7 illustrates two possible crosslinking processes of starch in basic conditions. One is crosslinked with epichlorohydrin by creating ether linkages,[61] and the other one is crosslinked with sodium trimetaphosphate by creating ester linkages.[52] The physical strength of starch is enhanced by introducing crosslinkers.[54,68] The size of SNPs can be controlled in the nanometer range through different crosslinking densities.

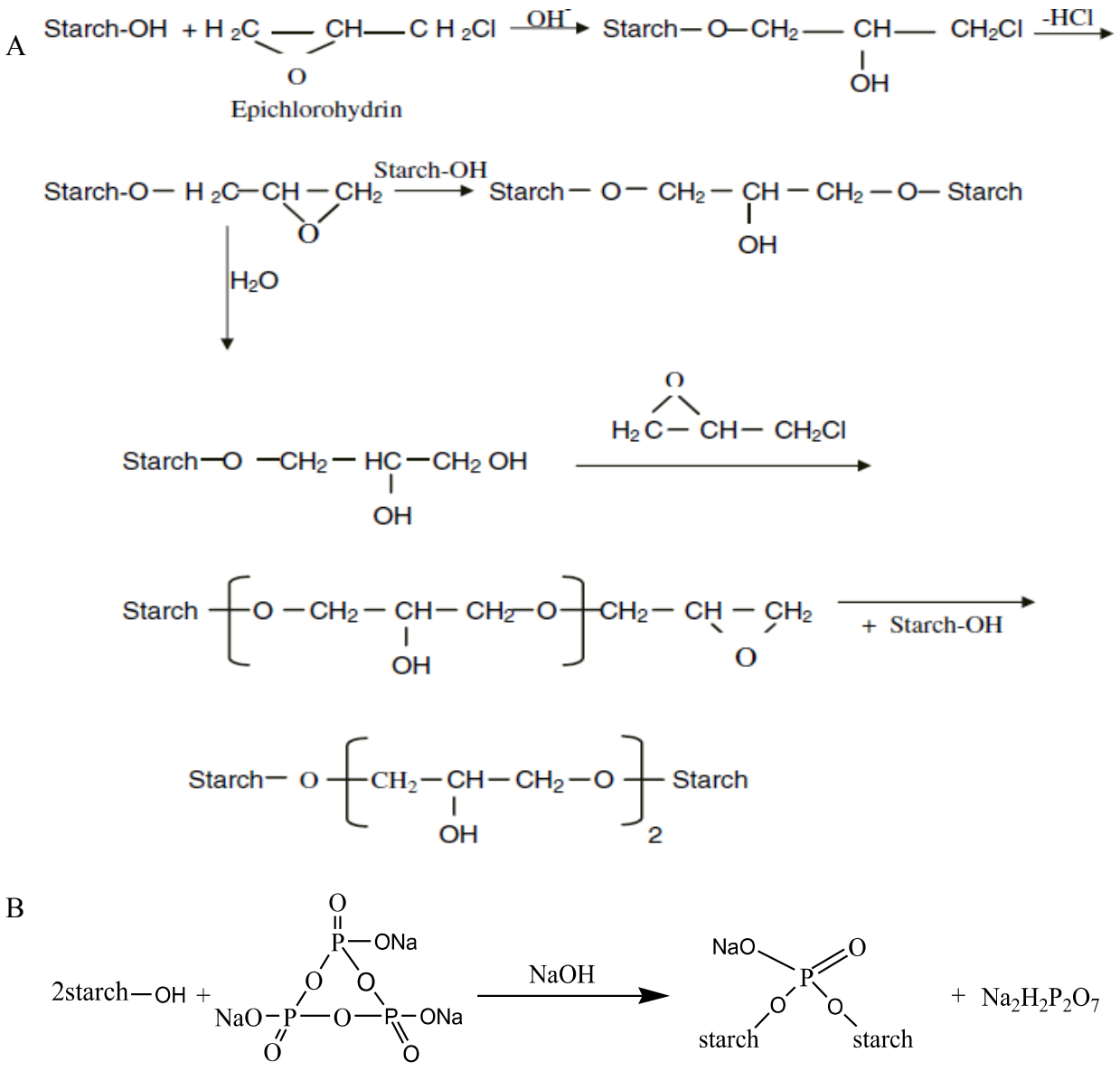

Figure 7. Two crosslinking process of starch using A) epichlorohydrin[61] and B) sodium trimetaphosphate[52] as crosslinking agents. Copyright 1999, Plenum Publishing Corporation.

These crosslinking reactions can be carried out in batch or continuously by reactive extrusion. As a traditional method, a batch process is performed in a vessel under continuous stirring. Since the native starch has poor solubility and high viscosity once it gels, relatively low starch concentration (35-45 wt%), high salt concentration (10-30 wt%) and low temperature (<

60 °C) are typically used in the batch process to overcome starch gelatinization.[69] Extra steps associated with additional cost are also needed to remove salt at the end of the process. Additional issues with the batch process are poor reaction selectivity and longer reaction time.[69] On the other hand, the extrusion process can overcome these problems. The extruder has a great mixing ability and is usually applied to deal with the high viscosity processes, such as those resulting from gelatinized starch.[70] Compared to the batch process, higher starch concentration (60-80 wt%) and higher reaction temperature (70-140 °C) can be handled in an homogeneous reaction medium.[69] As a result, the reaction rate is improved up to 15 folds over the batch process.[71] Twin screw extruders are generally preferred over single screw extruder, because of the extra screw designed to add reagent and remove by-products, which provides excellent control of mixing and short residence time (2-5 minutes).[69,70]

1.5.2.2 EcoSphere™ nanoparticles: preparation and structure

The SNPs used in my project were supplied by EcoSynthetix Inc. They were prepared by reactive extrusion on a large scale. They are produced by feeding a crosslinker and plasticizer to starch in a twin screw extruder and reacting the mixture at elevated temperature.[72,73] Solid starch nanoparticles finally exit the extruder as an agglomerate after water evaporates. The agglomerates of solid SNPs are shown in Figure 8.

Figure 8. EcoSphere™ starch nanoparticles agglomerate produced from extruder. Image is adapted from ref. [72]

The melting point of native starch is higher than its decomposition temperature.[74,75] As a result, plasticizer needs to be added to avoid starch decomposition.[73] The function of the crosslinking agent is to bind the starch chains together; therefore, they must have at least two sites to react with starch. In this case, glyoxal was used as crosslinking agent. Glyoxal can link starch nanoparticles together by reacting with the hydroxyl groups to form hemiacetals and acetals. Figure 9 illustrates the hypothesized crosslinking process of starch with glyoxal under acidic conditions. The possible structures of crosslinked SNPs are shown in Figure 10. It is worthy of note that the crosslinking process is reversible in aqueous solution. NMR techniques have been applied to characterize the crosslinkers in SNPs. Most glyoxal is involved in crosslinking but these crosslinkers can be partially released when crosslinked SNPs are dispersed in water.[76]

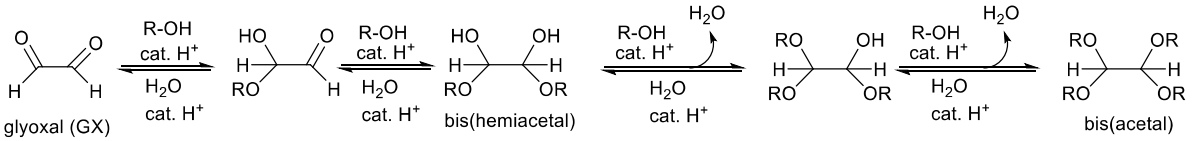

Figure 9. Crosslinking process of starch using glyoxal as crosslinking agent. R-OH is the hydroxyl groups on starch backbones.[76]

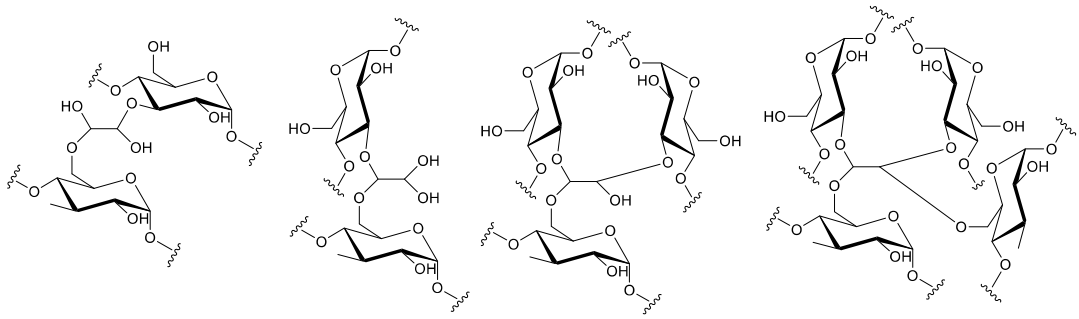

Figure 10. The possible structure of crosslinked SNPs.[76]

As a new nanomaterial, the structure and properties of SNPs need to be characterized. A hypothesized SNP structure is illustrated in Figure 11.[77] It has been proposed that the SNPs are bound together by intramolecular and intermolecular crosslinkers. The strucute of intermolecular crosslinker in SNPs is also shown in Figure 11. These intramolecular and intermolecular crosslinkers are believed to stabilize SNPs and decrease the swelling ratio of SNPs compared to native SNPs. The size of SNPs was reported by Gross's group[78] using dynamic light scattering (DLS).[78] Measurements were performed in DMSO and water. Their DLS results show that the size distribution of SNPs have two peaks around 45 and 300 nm in both solvent.[78] The smaller particles are attributed to the isolated starch nanoparticles; while the larger paticles are from the aggregated particles. The Gross's group also performed SEM to analyse the structure of SNPs (Figure 12), which is in good aggrement with DLS results.[79,78]

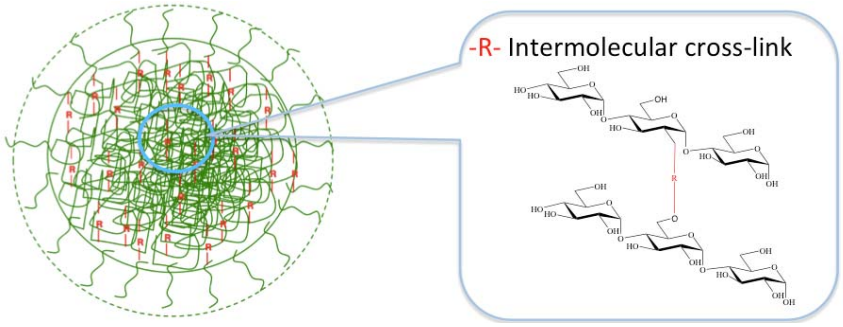

Figure 11. Hypothesized structure of crosslinked SNPs. [77]

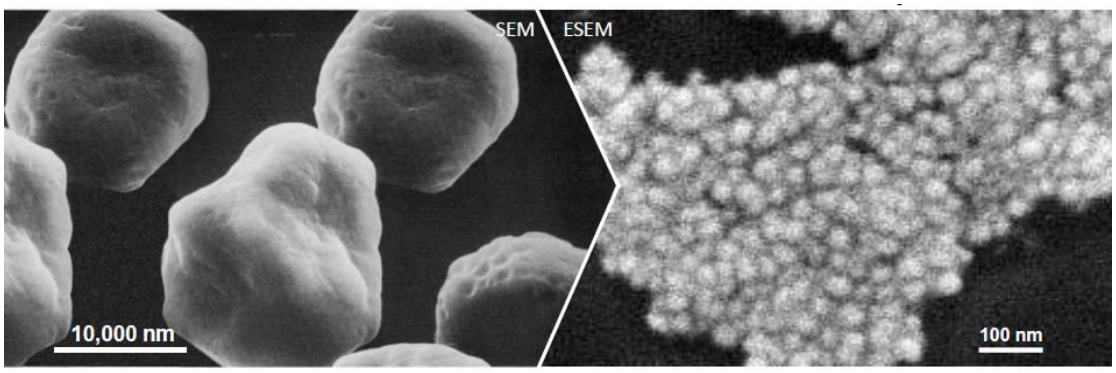

Figure 12. SEM of native starch granules and ESEM of EcoSphere™ starch nanoparticles. This figure is adapted from ref. [79] Copyright 2005, Elsevier Ltd.

1.5.3 Starch and starch nanoparticles for drug and gene delivery

1.5.3.1 Common modifications to starch and starch nanoparticles

With a poor solubility and high viscosity, starch has limited application in industry. Chemical modifications can improve certain properties of starch and add more functional groups to starch. Meanwhile, the abundant hydroxyl groups on glucose units making up the chain provide sites to be modified with multifunctional groups.[80,81] Consequently, various chemical modifications of starch have been studied. Three kinds of common modifications are anionic, cationic and hydrophobic modifications.

Anionic starch can be obtained by oxidizing hydroxyl groups of starch into carboxyl groups. The oxidation process is generally achieved by hypochlorite oxidation[82,83] and ozonation

oxidation.[84] Hypochlorite salt, as a traditional oxidation agent, is easy to handle in an industrial environment. However, hypochlorite oxidation has the obvious drawback of producing large amounts of salts that need to be disposed of.[85] On the other hand, ozone is a clean and powerful oxidation agent, which leaves no residues behind. But exposure to ozone can cause lung disease, which limits its application in industry and laboratory.[86] Another modification is via the addition of anionic groups to starch, such as carboxymethyl starch.[87–89] The present of carboxymethyl functional groups improves the solubility and reduces the gelatinization temperature of starch.[89] Carboxymethyl starch is widely used as a thickening, stabilizing, and water retaining agent to improve the quality of food.[88]

Cationic starch is commonly produced by introducing cationic groups onto the backbone. The cationic reagents containing amino, ammonium, sulfonium or phosphonium groups can be introduced via an etherification reaction with the hydroxyl groups of starch.[90–92] Conventionally, cationic starch is produced by etherification reaction of starch with quaternary ammonium groups.[92–94] Ammonium groups can be introduced by cationic reagents, such as glycidyl trimethyl ammonium chloride and 3-chloro-2-hydroxypropyltrialkylammonium chloride.[93,94] Their chemical structures are shown in Figure 13. Cationic starch is widely used as flocculants in wastewater treatment and additives in the paper industry.[43,91,46] Recently, it has been reported that cationic starch nanoparticles can be used as gene delivery vehicles.[94]

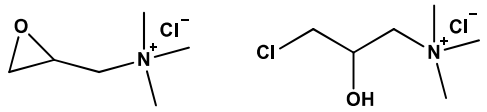

Figure 13. Chemical structure of glycidyl trimethyl ammonium chloride and 3-chloro-2-hydroxypropyltrialkylammonium chloride.

Chemical grafting is one of the most effective methods to produce hydrophobically modified starch with varied degrees of substitution.[58,95] Numerous papers have reported the esterification of starch with long chain fatty acids to produce hydrophobic starch material.[22,48-51] Of the various hydrophobic modifications, starch acylation has proved to be the most commercially effective and a relatively easy method.[99,100] Acylated starch is thermally stable and has lower gelatinization temperature compared to native starch.[99–101] The excellent properties of the acetylated starch have potential applications as surface coating,[100–102] and biomedical materials,[58,81,98] and in the packaging industry.[99,102]

1.5.3.2 Applications in drug and gene delivery

In the early stage, even though starch has the obvious advantages of being a biocompatible, biodegradable, and cost-effective material, only a few studies have reported on the applications of starch for drug delivery. The reasons come from the limitations of the structure and physical properties of native starch. The native polymeric chain structure of starch, which has a particle size range of 1 to 200 μm, requires modification techniques to reduce the size to the nanoscale. Unfortunately, early attempts by scientists only reduced the particle size to the micro-scale, which limited the efficacy of starch as drug delivery vehicles.[103,104]

As the emerging nanotechnology is moving at a fast pace, various nanoparticles have been tested as drug delivery vehicles and transferred to clinical practice in the past few decades. Due to the biocompatible advantages of starch, recent applications of SNPs derivatives as drug delivery platforms have attracted the interest of scientists. To become drug delivery vehicles, SNPs can be modified with various functional groups and added target ligands on their surface. Typically, the drug loading mechanisms include electrostatic attractions, hydrophobic interactions, coordination bonding and covalent conjugates.[80] Zhao and coworkers[105] reported

that the surface of SNPs can be conjugated with the active-targeting ligand folate modified with PEG. After the anticancer drug doxorubicin was loaded to modified SNPs, the targeting ability and inhibition effect to cancer cells were enhanced.[105] Additionally, hydrophobic polymer grafted SNPs[106] and di-aldehyde modified SNPs[67] are also reported to have efficient loading and sustained releasing abilities for Dox. Fatty acids grafted SNPs also have been found to be good drug delivery vehicles for hydrophobic drugs, which is reported to strengthen the efficacy of model anticancer drug indomethacin.[58] Furthermore, iron oxide impregnated SNPs are potential drug vehicles for magnetically targeted drug delivery.[62] Figure 14 A) describes the binding process of cisplatin to magnetic SNPs via coordination conjugation. Figure 14 B) describes the possible drug complexes release profiles in targeting infected cells obtained by applying an external magnetic field. These modified SNPs provide a possible pathway to target cancer cells, deliver drugs with higher efficacy, and minimize side effects.

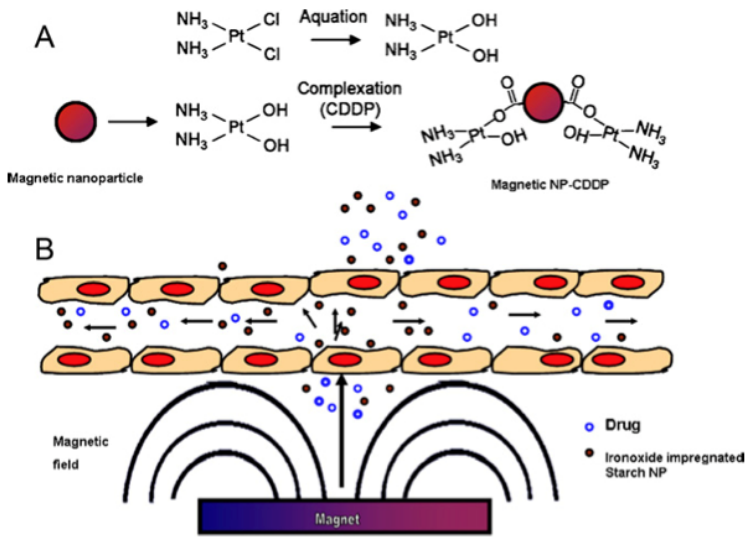

Figure 14. A) Binding process of cisplatin to magnetic SNPs and B) The possible drug complexes release profiles in targeting cells by applying an external magnetic field. This figure is adapted from ref. [62] Copyright 2012, Elsevier Ltd.

For gene delivery, since unmodified SNPs do not interact with DNA strongly, the straightforward method to increase DNA affinity is via cationic modification of starch. One type of reported cationic modification is to graft the cationic biocompatible polymer polyethylenimine (PEI) to the surface of oxidized SNPs. The starch-graft-PEI synthesized by Lehr et al. achieved lower toxicity and better transfection efficacy of plasmid DNA than free DNA.[107] Cationic groups can be added directly onto starch backbone. Recently, Kost and coworkers[94] developed SNPs modified with a quaternary ammonium group for siRNA delivery. Their results show that the SNPs/siRNA complexes resulted in effective cellular uptake.

1.6 Thesis objectives

The goal of this research is to modify SNPs for drug and gene delivery. SNPs are a new material produced by EcoSynthetix Inc. in an industrial scale. So far SNPs are only being commercially used for paper coating. Since the safety of nanomaterial is a great concern for biomedical applications, one of this thesis objectives is to study the toxicity of unmodified and modified SNPs. In particular, my thesis focuses on the toxicity of SNPs and the methods that can be applied to eliminate this toxicity. Meanwhile, the safe concentration range of SNPs used for drug and gene delivery was also tested and analyzed. In order to balance the safety and efficacy of a drug delivery system, the amount of modified SNPs employed as vehicles needs to be carefully controlled. Doxorubicin, an effective anticancer drug, is used as the model drug to be loaded onto modified SNPs. Therefore, the second objective of this thesis is to synthesize and characterize carboxyl-modified SNPs for doxorubicin loading. Finally, the cationic SNPs developed by Duncan Li in Dr. Taylor laboratory were characterized and utilized for DNA delivery.

In summary, the specific objectives of this thesis for drug delivery are:

1. Study the origin of the toxicity of EcoSphere™ starch nanoparticles

2. Synthesize and characterize oxidized SNPs with different oxidation levels

3. Evaluate the effect of oxidation and washing on the toxicity of SNPs

4. Investigate Dox loading properties

5. Study Dox release from carboxylated SNPs

6. Test the toxicity of drug conjugate and compare to free drug

The specific objectives of this thesis for gene delivery are:

1. Characterize cationic SNPs with different degrees of substitution

2. Evaluate the effect of degree of substitution on the toxicity of cationic SNPs and compare the toxicity to other commercial gene transfection agents

3. Investigate DNA binding to cationic SNPs

4. Deliver DNA to cancer cells

Chapter 2 Toxicity of SNPs from EcoSynthetix and oxidized SNPs

2.1 Introduction

As SNPs are produced commercially by EcoSynthetix Inc. for paper coating, it is essential to investigate the safety aspect of the SNPs as drug delivery vehicles. In this chapter, the cytotoxicity of the unmodified SNPs supplied by EcoSynthetix Inc. was investigated. The reasons for the toxicity of the SNPs and the development of a methods to eliminate the toxicity were addressed. Additionally, the dose range of the modified SNPs used for drug delivery need to be carefully controlled in order to balance the safety and efficacy of the drug delivery system.

In this study, a HeLa cell line was chosen to test the toxicity of SNP samples. HeLa is the first immortal cell line harvested from a cancer patient. Their robustness allows them to grow in a wide range of conditions.[108] HeLa cell lines are widespread in the scientific community due to their robustness and fast replication every 24 hours.[109] To test the safety of the SNPs as drug delivery vehicles, SNPs need to be incubated with cancer cells for an appropriate time to quantify cell viability.

Cell viability can be measured via various assays. These automated methods are required to be sensitive, quantitative and reliable. The MTT assay is a standard colorimetric assay to quantify cell viability in high throughout, which is based on the conversion of yellow tetrazolium salt MTT into purple insoluble formazan by living cells.[90] Live cells have reductase enzymes in mitochondria and these enzymes can reduce the yellow tetrazolium salt called 3-(4,5-dimethylthiazol-2-yl)-2,5-diphenyltetrazolium bromide (MTT) into insoluble MTT formazan with a purple colour (Figure 15). This colour conversion occurs only when reductase enzymes in mitochondria are active. Therefore, the resultant colour is proportional to the number of the live cells.[112,113] The absorbance at a specific wavelength can be quantified using a microplate reader.

The MTT assay has advantages of being less time consuming and cheap and having a relatively high throughout.[91] The viable cells in 96-well plates can be measured via the fluorescence plate reader without the need for elaborate cell counting.[91] In this research, all cell viability and toxicity are therefore measured via the MTT assay.

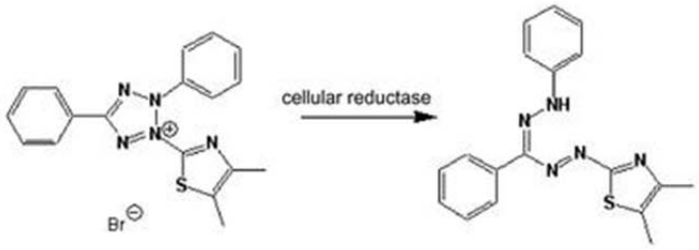

Figure 15. The conversion of yellow tetrazolium salt MTT into insoluble formazan via reductase enzymes. [113]

2.2 Effect of crosslinker concentration on the toxicity of SNPs from EcoSynthetix

SNPs with different crosslinking densities were obtained from EcoSynthetix Inc. These SNPs were prepared using reactive extrusion and are available in an industrial scale. Firstly, the toxicity of the SNPs with different crosslinking densities was tested. SNPs with 0%, 1%, 3%, 5% (w/w) crosslinker densities are abbreviated as GX0 GX1, GX3, GX5, respectively. "GX" represents the crosslinking agent glyoxal used by EcoSynthetix. Figure 16 shows the toxicity of the unmodified SNPs with different crosslinking densities. It shows that the SNPs with more crosslinkers have higher toxicity. In other words, the crosslinker might be the source of the toxicity of SNPs. In the manufacturing of SNPs, the amount of glyoxal as crosslinker added to GX0 to GX5 increases with the increasing crosslinking density. My co-worker Duncan Li used NMR techniques to characterize the crosslinkers in the unmodified SNPs. He found that free glyoxal molecules can be detected by NMR when the SNPs are dispersed in water and the amount of free glyoxal molecules calculated from the NMR spectra is less than that used in the

manufacturing of SNPs.[76] According to these results, these free glyoxal molecules might have two sources: 1) a fraction of the glyoxal molecules are not involved in the crosslinking process of SNPs; 2) a fraction of the glyoxal molecules are released from the crosslinked SNPs when dispersed in water due to the reversible crosslinking reaction.

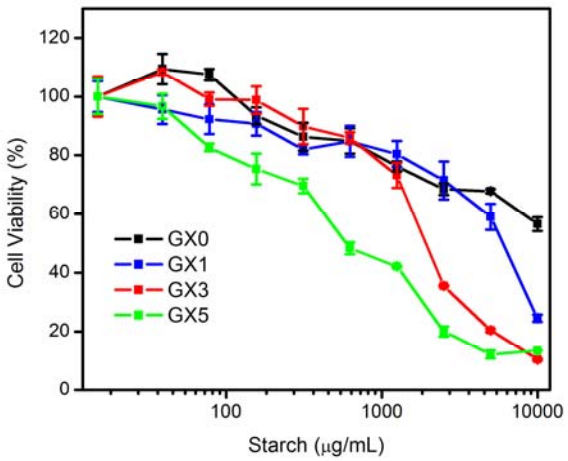

Figure 16. The effect of crosslinking density on the toxicity of unmodified SNPs.

To confirm the source of toxicity, we compared the toxicity of the GX0 sample spiked with an amount of glyoxal equal that used to prepare GX5 from EcoSynthetix. Figure 17 shows that the spiked GX0 sample has a trend similar to the actual GX5 sample from the company. As mentioned above, the amount of free glyoxal molecules detected from the NMR spectra is less than that used in the manufacturing of SNPs; while the amount glyoxal used to spike GX0 is the same as what is supposedly used in the manufacturing of GX5. As a result, the GX5 sample has slightly lower toxicity than the spiked GX0. These toxicity experiments confirmed that the free glyoxal molecules are at the origin of the toxicity of the unmodified SNPs.

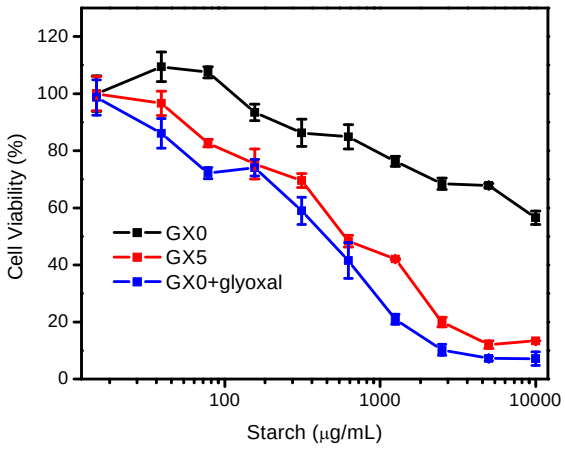

Figure 17 Toxicity of spiked GX0 (GX0+glyoxal) and actual GX5 from the company.

The mechanism of gyoxal toxicity was investigated for the first time by O'Brien et al. by studying the cytotoxic effect of gyloxal in isolated rat hepatocytes.[114] The mechanism of gyoxal toxicity proposed by O'Brien et al. is shown in Figure 18.[114] Briefly, glyoxal can induce lipid peroxidation (LPO) causing the formation of reactive oxygen species (ROS). Since glutathione (GSH) plays a protective role against ROS, excess ROS can lead to a decrease of GSH levels in cells. GSH also works as a catalyst in the production of glycolate. Consequently, decreased GSH level can decrease glycation leading to the collapse of the mitochondrial membrane. Finally, decreased GSH leads to more ROS formed which leads to more LPO. The formaldehyde formed in the LPO process could open the mitochondrial permeability transition pore (MPTP) to release cytochrome c and activate caspases, which lead to cell death.[114] O'Brien et al. also reported that the cytotoxicity of glyoxal in rat hepatocytes depended on dose and time.[114] The glyoxal toxicity was also studied in lung epithelial cell lines L132 NAD[115] and E1A-NR3.[116] The cytotoxicity of glyoxal is relatively lower in rat hepatocytes cell lines[114] compared to that in lung epithelial cell lines L132 NAD[115] and E1A-NR3.[116]

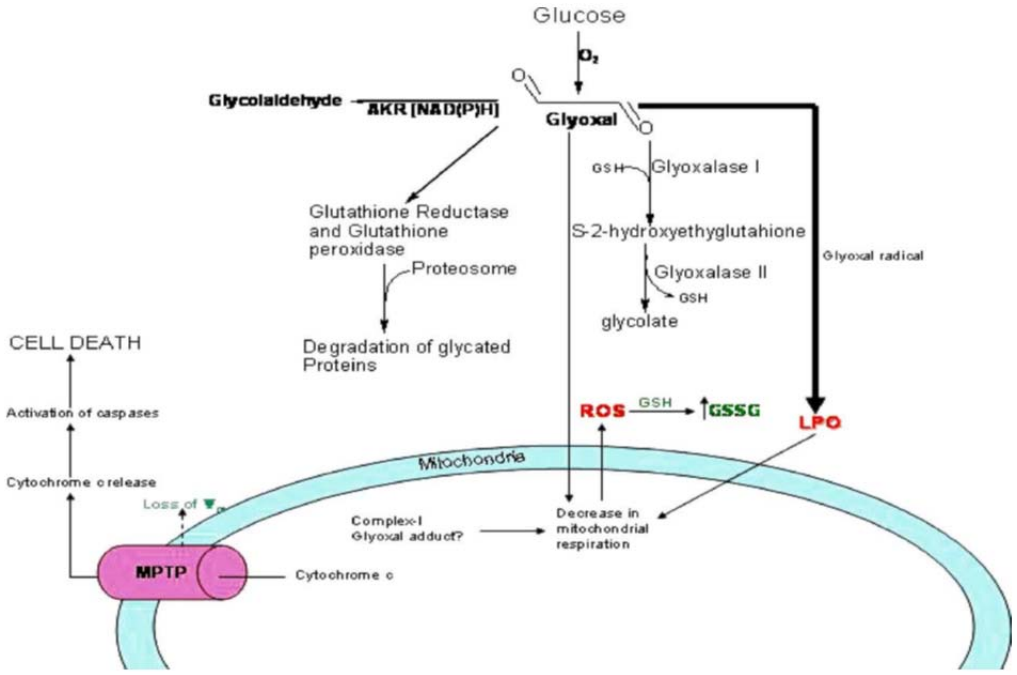

Figure 18. The mechanism of glyoxal toxicity proposed by O'Brien et al.[114] Copyright 2004, Elsevier Inc.

Although the concentrations range of glyoxal (8 mM) used in the toxicity study of GX5, which represents the highest amount of glyoxal used to prepare the SNPs, is slightly higher that in isolated rat hepatocytes (5 mM) and lung epithelial cell lines (0.8 mM), the cytotoxicity effect of glyoxal in the HeLa cell lines is in good agreement with that in other cell lines.[115,116] Knowing the cytotoxicity effect of glyoxal in cancer cells will help researchers to choose more suitable and safe crosslinking agents in the future manufacturing of SNPs.

2.3 Effect of oxidation and washing on the toxicity of SNPs

Doxorubicin (Dox) is used as the model drug in my research. For Dox delivery, drug delivery vehicles with a slight negative charge are typically perferred due to the positive charge

of Dox. Since SNPs are neural particles covered by hydroxyl groups, the hydroxyls can be oxidized into carboxyls with negative charges to achieve successful drug loading. Since SNPs can be precipitated out in ethanol, the washing process was performed in ethanol followed by centrifugation. As a result, the impurity and free glyoxal molecules can be separated into the supernatant and removed from the SNPs by ethanol washing. After oxidation and further washing, the oxidized SNPs with different crosslinking densities are almost non-toxic as shown in Figure 19.

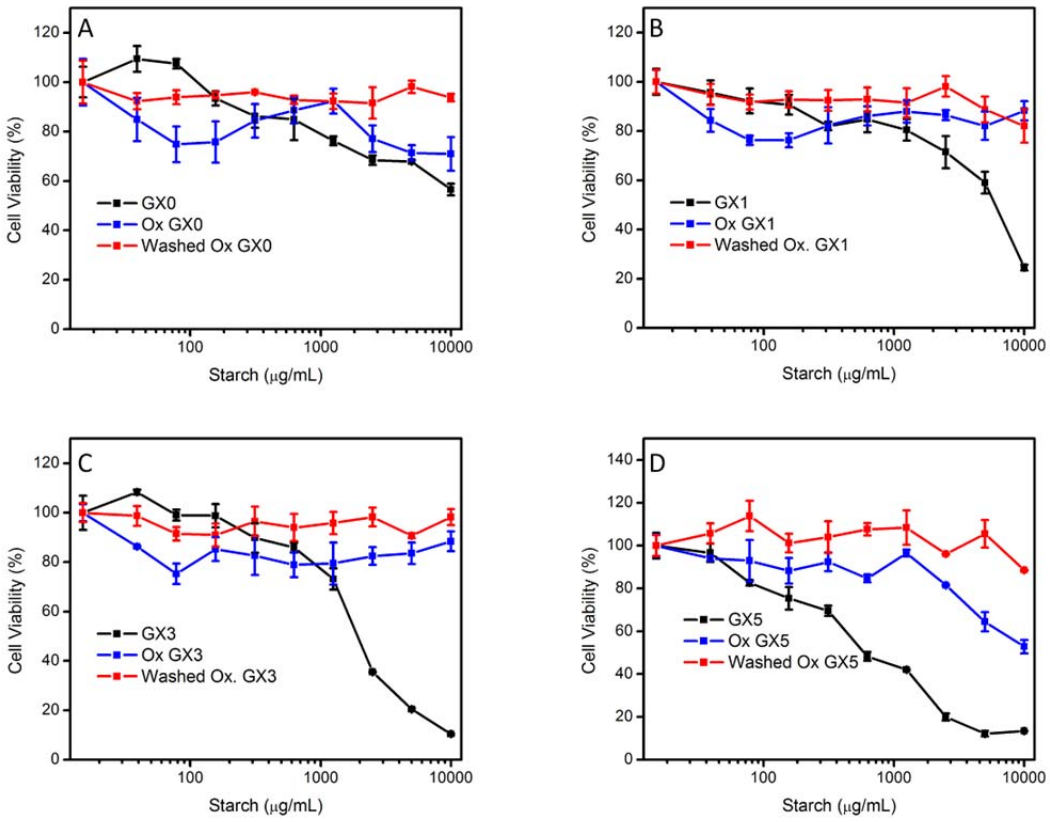

Figure 19. The effect of oxidation and washing on the toxicity of A) GX0, B) GX1, C) GX3, and D) GX5.

2.4 Summary and future work

In this chapter, the toxicity of the unmodified and modified SNPs in the HeLa cell line was investigated by the MTT assay. The free glyoxal molecules were found to be the reason for the toxicity of unmodified SNPs. However, toxicity can be eliminated by the washing process. Finally, the washed and oxidized SNPs are almost non-toxic, which can be considered safe to deliver cancer drugs.

Future studies can focus on the source of free glyoxal molecules. If some of the glyoxal molecules are not involved in the crosslinking process in the manufacturing of SNPs, the amount of glyoxal molecules actually involved in the crosslinking process should be determined. If the crosslinking process is reversible and glyoxal can be partially released from crosslinked SNPs when dispersed in water, the factors affecting the reversible crosslinking reaction and the methods to avoid or slow the reversible crosslinking reaction should be investigated. Since the toxicity of glyoxal has already been studied and reported by scientists, EcoSynthetix could employ more stable and safer crosslinking agents for the future development of SNPs for pharmaceutical applications.

2.5 Materials and methods

2.5.1 Materials

SNPs with different crosslinker densities were provided by EcoSynthetix Inc. (Burlington, ON, Canada). The crosslinker densities were 0%, 1%, 3%, and 5% (w/w) of SNPs, and these SNPs were abbreviated as GX0 GX1, GX3, GX5, respectively. “GX” means that the crosslink agent used by EcoSynthetix Inc. was glyoxal. DMF, SDS, MTT, 2,2,6,6-tetramethyl-1-piperidinyloxy (TEMPO), NaBr, and 5% NaClO (bleach) were purchased from Sigma–Aldrich (St Louis, MO). HEPES, NaOH, NaCl and DMSO were from Mandel Scientific (Guelph, ON,

Canada). Aqueous solutions were prepared using Milli-Q water (18.2 MΩ resistivity). HeLa cell line (CCL-2^{TM}) was obtained from the American Type Culture Collection (ATCC, Manassas, Virginia) through the help of the laboratory of Dr. Shirley Tang (Waterloo, Ontario, Canada).

2.5.2 SNP oxidation and washing

The TEMPO-mediated oxidation of SNPs followed the protocol in the literature reported by Kato et al.[82] The primary hydroxyl groups in the glucose unit of SNPs can be selectively oxidized into a carboxyl groups. 5% (w/w) SNPs was dispersed in 50 mL of Milli-Q water, then mixed with 23.75 mg TEMPO and 317.5 mg NaBr under stirring. Then SNPs was oxidized by the gradual addition of 5% NaClO (bleach) in an ice-water bath. TEMPO worked as a catalyst in the oxidation process. After each addition of the oxidant NaClO (5% bleach), the pH increased slightly before being followed by a steady decrease. For the reaction to proceed, the pH must be maintained around 10.75 by adding additional 0.5 M NaOH. The level of oxidation was determined based on the amount of NaOH used to produce carboxyl groups. For 20% oxidation, a total of 5 mL NaOH and 6.6 mL of NaClO was added gradually. Then the reaction was quenched by the addition of 3-fold ethanol to the mixture. Once oxidized SNPs were precipitated out in ethanol, the precipitate was centrifuged to remove the supernatant. Then the yellowish pellet was re-dispersed in water and re-precipitated in ethanol. This process was carried out three times.

2.5.3 Cytotoxicity study of SNPs

Cell culture. In this research, a HeLa cell line was used as the cancer cell model to study the toxicity of SNPs. The HeLa cell line was cultured in DMEM/F12 medium containing 10% v/v fetal bovine serum (FBS), 10% v/v of 100 U/mL penicillin-streptomycin, and kept in a humidified 5% CO_2 incubator at 37 °C.

MTT assay. The toxicity of SNPs with different crosslinker densities was evaluated using the MTT assay. Firstly, 100 μL of HeLa cells suspension in DMEM/F12 cell medium was seeded at densities of around 5,000 cells per well in 96-well plate (costar), followed by the incubation for 24 h in 5% CO_2 and 95% humidified cell incubator at 37 °C. After 24h incubation, the stock solution of SNPs (5% w/w in water), oxidized SNPs, and washed SNPs with different crosslinker densities (0%, 1%, 3%, and 5% w/w) were diluted to the desired concentrations. The culture medium was removed and replaced with 100 μL of freshly prepared culture medium containing various SNP samples. The cells were further incubated with samples for 72 h in the cell incubator. Next, 5 mg/mL of MTT stock solution was prepared in PBS. The culture medium was removed and replaced with 100 μL of freshly prepared culture medium. 25 μL of MTT stock solution was added to each well of the treated cells except blank wells. 25 μL of PBS was added to the wells with untreated cells as control groups. After the plates were incubated for 2 h in the cell incubator, 100 μL of extraction buffer (20% SDS in 50% DMF, pH 4.7) was added to each well and then incubated for 4 h in the cell incubator. The absorbance of the resultant purple colour was measured at 570 nm using a microplate reader (SpectraMax M3). All the wells were prepared in triplicate. Cell viabilities were averaged and normalized to the untreated cells, which worked as negative controls cultured in the cell medium without sample added.

Chapter 3 TEMPO oxidized SNPs for drug loading

3.1 Introduction

In this chapter, the capability of oxidized SNPs for drug loading was evaluated. Doxorubicin (Dox) was used as the model drug. As an effective clinical anticancer drug, Dox also has significant side effects. It is necessary to develop targeted delivery vehicles to decrease the toxic effects to the healthy tissues. Many materials have been tested for this purpose and the approved platforms so for include liposomes and biodegradable polymers. However, the synthesis processes of these vehicles are complicated and not cost-effective. Compared to these delivery platforms, our SNPs are renewable and can be produced on an industrial scale. Due to the positive charge of doxorubicin hydrochloride (Dox•HCl), negatively charged vehicles are supposed to enhance the drug loading capacity. Therefore, SNPs need to be modified with anionically functional groups to achieve drug loading. Since the main constituents of SNPs are glucose units, the chains of SNPs contain many hydroxyl groups. By TEMPO-mediated oxidation, the primary hydroxyl moieties of the SNPs can be oxidized into carboxyl groups. After oxidation, Dox can be loaded onto carboxyl SNPs by electrostatic interactions. The drug adsorption and release profiles can be investigated. Finally, the efficacy of the drug complexes was tested and compared with free Dox.

3.2 TEMPO oxidation of SNPs

To introduce carboxylic acids, TEMPO-mediated oxidation was used to selectively oxidize SNPs. The key advantage of TEMPO oxidation is its selective oxidation toward primary hydroxyls (C6 position in Figure 20). The selective oxidation of polysaccharides by TEMPO-mediated was firstly reported by Nooy et al.[117] A subsequent study of selective oxidation on starch was performed by Kato et al.[82] They examined the oxidation process in detail and

proposed a two-step oxidation mechanism. They suggested that hydroxyl groups are first oxidized into aldehydes, and then NaOH activates the carbonyls to form intermediates for the second oxidation into carboxylic acids as shown in Figure 20.

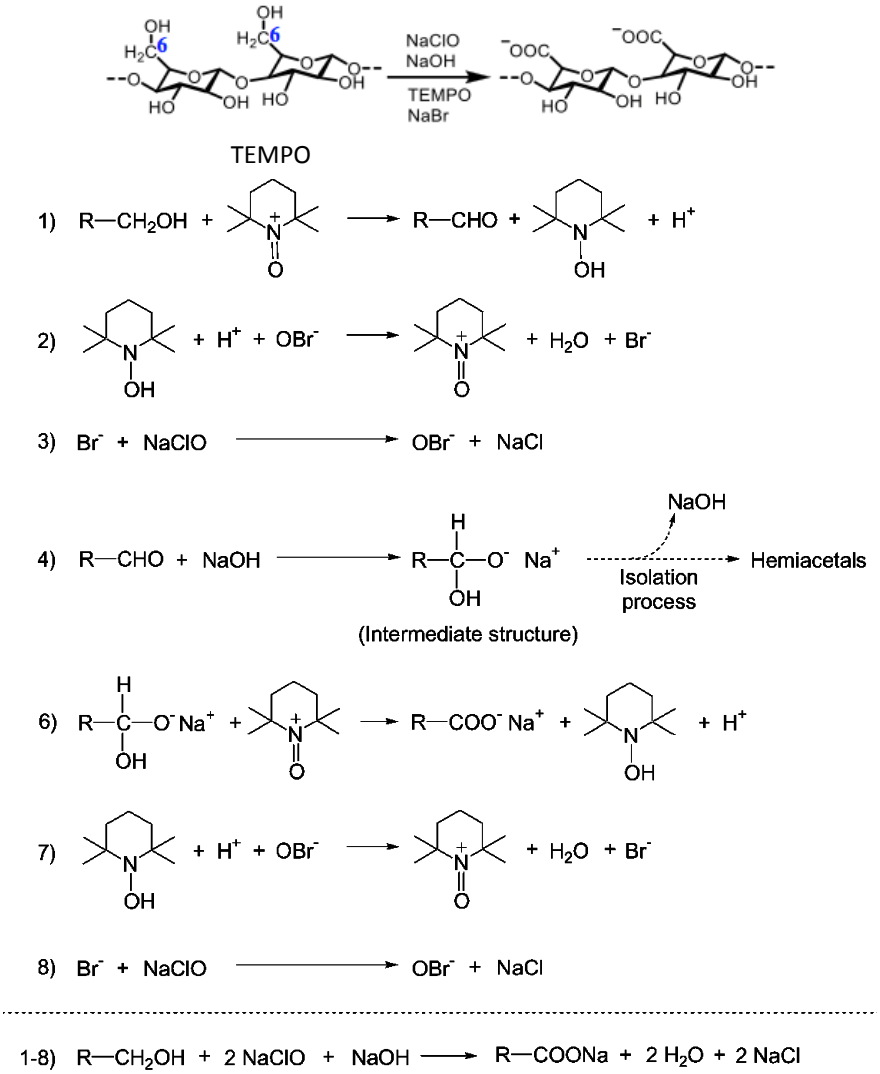

Figure 20. Brief and detailed scheme of TEMPO-mediated oxidation of SNPs.[82] R-OH stands for the primary hydroxyl groups on SNPs.

The structure and catalytic action of TEMPO (2,2,6,6-tetramethylpiperidine-1-oxyl) is shown in Figure 20. Each glucose unit has a primary hydroxyl at the C-6 position, while other

hydroxyls are secondary. Using TEMPO as a catalyst, only the primary hydroxyls at the C-6 position can be oxidized into carboxylic acids.[83] The oxidation also requires NaBr as a co-catalyst and NaClO as an oxidation agent. A controlled amount of NaClO was added to allow for the oxidation of SNPs. The oxidation proceeded with a corresponding pH drop. Meanwhile, the pH needed to be maintained around 10.75 by adding NaOH for the reaction to proceed. As shown in Figure 20, each mole of NaOH consumed is supposed to produce a molar equivalent of intermediate structures, which are then completely oxidized into C6 carboxyls. As a result, the level of oxidation is controlled by the amount of NaOH consumed to reach the final neutral pH. Different oxidation levels of SNPs (1, 2, 5, 10, and 20%) were synthesized to investigate the effect of oxidation level on drug loading capacity.

3.3 Spectroscopic characterization of oxidized SNPs

3.3.1 UV-vis absorption spectroscopy of SNPs

To confirm the oxidation extents of SNPs, the UV-vis absorption spectra of different oxidation levels of SNPs (1, 2, 5, 10, and 20%) were measured. Figure 21 shows the UV-vis spectra of SNPs at different oxidation levels and the change of SNP peak intensity at 253 nm as a function of oxidation level. As shown in Figure 21A, the non-oxidized SNPs does not show any peak from 220 nm to 600 nm. With just 1% oxidation, an intense peak at 253 nm can be observed, which is assigned to the absorbance of the newly generated aldehydes which are oxidation intermediates. TEMPO-mediated oxidation of SNPs proceeds via a two-step mechanism at the primary hydroxyl group; the first oxidation converts the hydroxyl into an aldehyde, while the second oxidation converts the aldehyde into a carboxylic acid as shown in Figure 20. This peak intensity doubles with 2% oxidation. Beyond 2% oxidation, the peak growth slows down, with barely any change being observed from 5 to 20% oxidation. After that,

the peak starts to decrease with further increase in oxidation. With 100% oxidation, the peak has completely disappeared. Figure 21B shows the absorbance of the oxidized SNPs at 253 nm which was assigned to the aldehyde groups that are intermediates during the oxidation reaction. When the oxidation level was increased from 1% to 5%, a large amount of aldehyde groups was produced. However, when the oxidation level is increased from 5% to 20%, the rate of aldehyde generation is similar to that of their conversion into carboxylic acids, resulting in a flat aldehyde concentration in this oxidation range. Once the oxidation level is higher than 20%, the second TEMPO oxidation step dominates. The aldehydes are converting into carboxylic acids more quickly than they are generated. The concentration of aldehyde groups starts to decrease with further oxidation. At 100% oxidation, all aldehydes are converted into carboxylic acids.

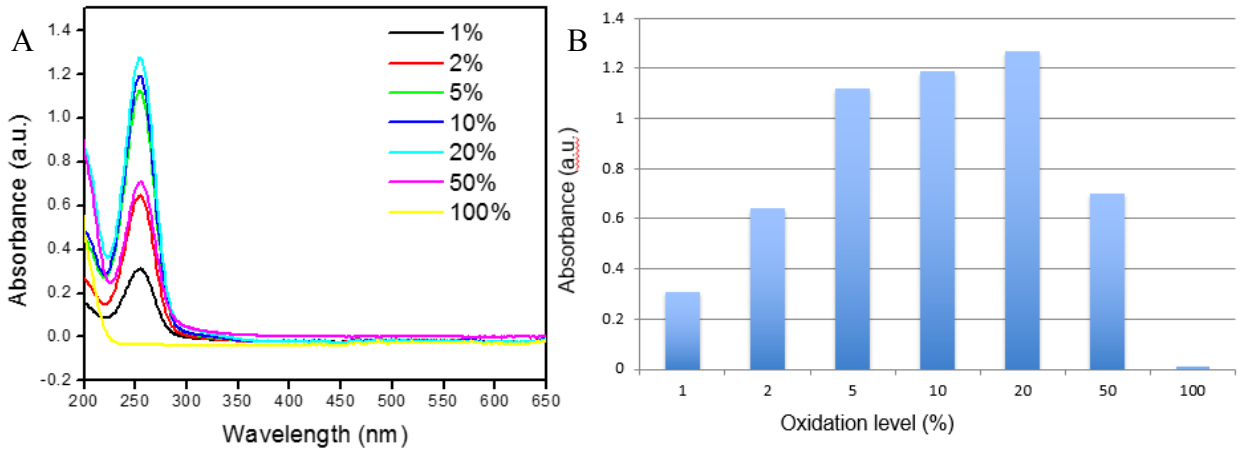

Figure 21. A)UV-vis spectra of SNP at different oxidation levels. B) the change of SNP peak intensity at 253 nm as a function of the oxidation level.

3.3.2 Physical properties of oxidized SNPs

To understand the property of the oxidized products, my co-worker Howard Tsai measured the variations in nanoparticle size and surface charge after TEMPO oxidation. Dynamic light scattering (DLS) was used to measure the size distribution of the SNPs. Results

showed that the hydrodynamic diameter (D_h) of the unmodified SNPs is 20 to 30 nm, which is in good agreement with previous findings.[118] The 1%, 2%, and 5% oxidized SNPs have a particle size around 10 nm. Compared with the non-oxidized SNPs, the decreased size suggested the some level of degradation during the oxidation process. SNPs with oxidation levels equal to 10% and 20% have a broad size distribution from 10 nm to 130 nm. To explain the broad size distribution, we proposed that the small fragments of degraded SNPs aggregate via hydrogen bonding networks of different sizes. Higher levels of oxidized SNPs have more carboxyl groups to hydrogen-bond with SNPs hydroxyls, resulting in a broader size distribution.

The ξ-potential measurements were used to measure the surface charge of SNPs after oxidation. Unmodified SNPs showed a potential close to zero due to its non-charged hydroxyl groups on the surface. With increasing oxidation level, the ξ-potentials of oxidized SNPs gradually decreased at basic conditions, reflecting a gradual increase in negative charge on the surface of the oxidized SNPs. As expectated, carboxylate anions are present on the SNP surface under basic conditions. Higher oxidation levels of SNPs with more carboxylate anions can result in higher negative surface charge.

3.4 Oxidized SNPs for doxorubicin loading

3.4.1 Doxorubicin and its delivery

Doxorubicin (Dox) is one of the most effective anti-cancer drugs. The structure of doxorubicin hydrochloride (Dox•HCl) is shown in Figure 22. Dox can directly intercalate DNA and stop the process of replication, eventually leading to apoptosis.[119] In addition, the orange fluorescence of Dox makes it easy to quantify and track. However, the side effects of Dox are of great concern. Dox not only kills cancer cells, but also can accumulate in healthy tissues such as heart, liver, spleen, and bone marrow.[119] The major drawbacks of Dox are the poor bio-

distribution and low selectivity for targeting cancer cells. Due to the widespread distribution of Dox in the whole body, the amount of Dox reaching the targeted cells is not sufficient to kill cancer cells. As a result, dosage has to be increased. However, the high doses of drugs also enhance the risk to normal tissues.[120] In addition, the solubility of Dox needs to be enhanced to reduce its precipitation in the aqueous circulation system.[119] Therefore, it is important to develop drug delivery vehicles for Dox to target cancer cells and decrease the damage of healthy tissues.

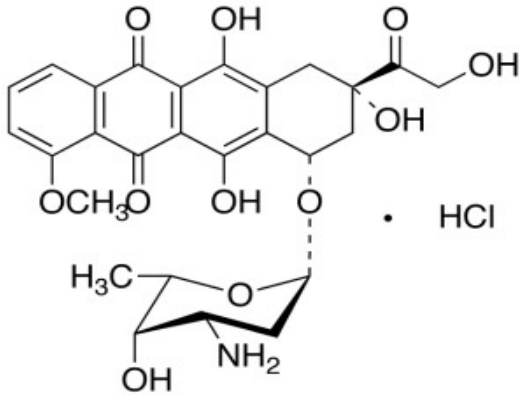

Figure 22. Structure of doxorubicin hydrochloride (Dox•HCl).

Various drug delivery platforms have been reported for Dox delivery in the last few decades. Doxil® is a doxorubicin loaded poly(ethylene glycol) coated (PEGylated) liposome, which was approved by FDA in 1995 and reached the market for the treatment of ovarian and breast cancer.[121,122] PEG, as a biocompatible polymer, coats the surface of liposome to ensure its stability and protect drugs from the immune response. Studies have shown that a PEGylated liposome has a prolonged circulation in the blood and can release Dox in a controlled manner.[122] Other biocompatible nanomaterials, such as polysaccharides, have also been involved as nanocarriers for Dox delivery. Effective controlled and sustained release profiles of Dox from

PEG-modified dextran NPs[123] and pH-responsive dextran-g-cholesterol micelle[124] have been reported. Active targeting delivery of Dox is also achieved using targeting ligands conjugated to SNPs[105] and dextran NPs[125] via receptor-mediated pathways. Among these platforms, vitamin folic acid (folate) has been widely used as target ligand because of its selectivity to breast and ovarian cancer cells.[105,125–127]

3.4.2 Adsorption of Dox

After Dox has been adsorbed onto the oxidized SNPs by electrostatic interactions, an obvious fluorescence quenching of Dox was observed. Therefore, Dox adsorption onto SNPs can be monitored using fluorescence quenching. To systematically study the adsorption mechanism, the fluorescence of Dox was monitored when Dox was titrated with the oxidized and non-oxidized SNPs. Figure 23A and 23B illustrate the intensity and shape changes of the fluorescence emission spectra during the Dox titration process by the oxidized and non-oxidized SNPs. Figure 23C plots the fluorescence peak intensity change of Dox at 550 nm as a function of the concentration of the SNPs. Figure 23D plots the fluorescence quenching efficiency of Dox as a function of the concentration of the SNPs. As shown in Figure 23C, for the oxidized SNPs, the fluorescence intensity of Dox gradually decreases with increasing concentration of the oxidized SNPs. In the case of Dox titrated with non-oxidized SNPs, no obvious fluorescence quenching is observed unless the concentration of SNPs was very high. As shown in Figure 23D, the quenching efficiency of oxidized SNPs is higher than that of non-oxidized SNPs at the same concentration. Since the functional groups on the non-oxidized SNPs are unlikely to interact with Dox, Dox may be just physically trapped by the SNPs. This trapping is attributed to the gel-like structure of the unmodified SNPs.

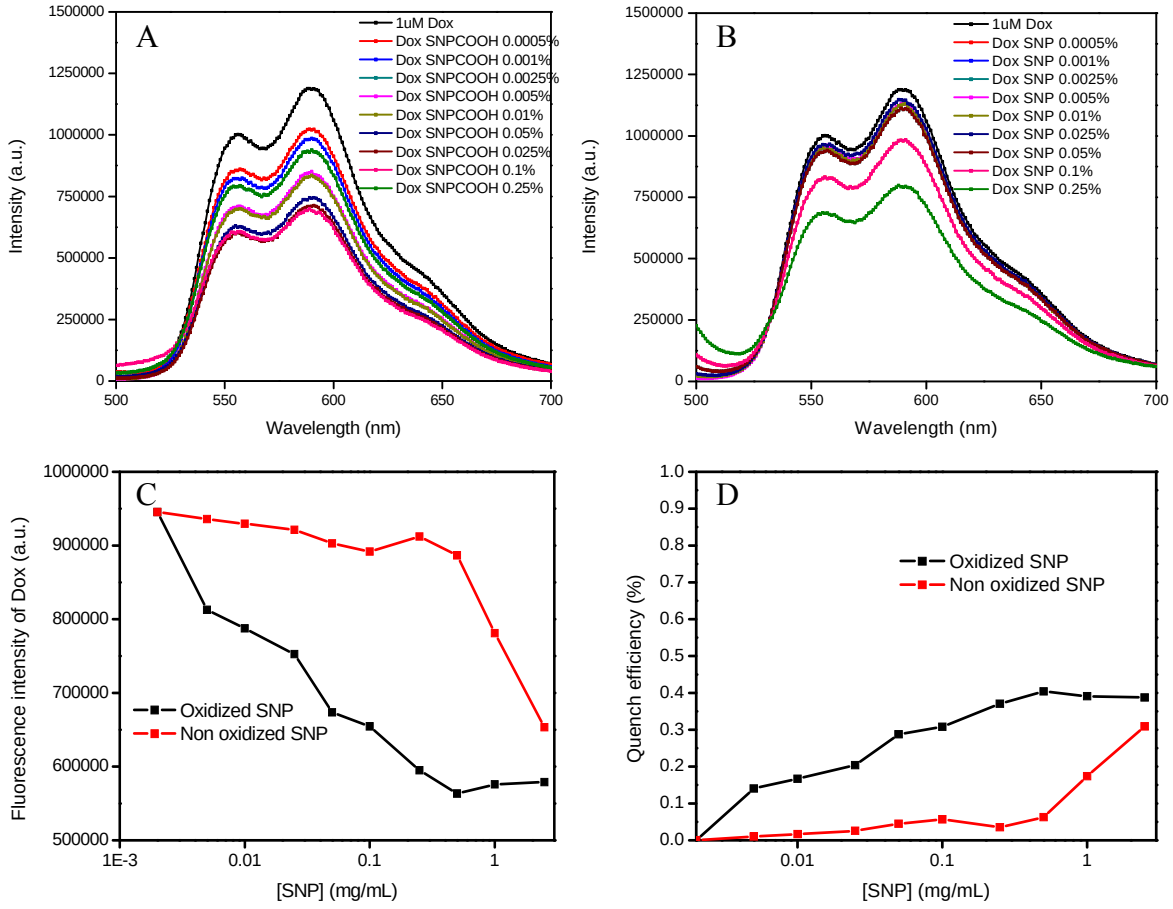

Figure 23. Dox titration process with oxidized SNP or non-oxidized SNP: Fluorescence emission spectra of Dox in different amounts of A) oxidized SNPs and B) SNPs ; C) Fluorescence peak intensity change at 550 nm as a function of SNP concentration; D) Fluorescence quenching efficiency of Dox as a function of SNP concentration.

These titration experiments indicated oxidized SNPs with carboxyls can strongly adsorb cationic Dox by electrostatic interactions, while the non-oxidized SNPs can only physically trap Dox in the gel-like structure of the SNPs. This conclusion is further supported by experiments conducted with granular starch. These micrometer sized starch particles were involved because they can be easily precipitated out by centrifugation. We used granular starch and its oxidized

product to adsorb Dox. After the precipitation of granular starch and oxidized granules, we compared the fluorescence intensity of Dox in the supernatant with or without granular starch. We observed that no adsorption of Dox occurred with the normal starch granules but adsorption occurred with oxidized granules. Therefore, we proposed that Dox might be only physically trapped by the unmodified SNPs due to their gel-like structures; while oxidized SNPs can strongly bind Dox by electrostatic interactions. After adsorption, Dox molecules might aggregate to cause self-quenching.

3.4.3 Release kinetics of Dox

To measure the drug release profiles, Dox was loaded onto the unmodified SNPs and the oxidized SNPs. Released drugs were separated from SNPs using dialysis tube with a molecular weight cut off of 5,000. The release profiles of Dox are shown in Figure 24. The release of free Dox is compared with that of Dox loaded with oxidized SNPs and unmodified SNPs. The initial intensity is close to zero, indicating that little free drugs are present and the loading capacity is very high. Both free Dox and Dox in unmodified SNPs have a burst release in the first 7 hours. After 1 day, 90% of the initial amount of free Dox loaded into the dialysis tube was released; meanwhile, 50% of the initial amount of Dox with unmodified SNPs loaded into the dialysis tube was released. This result implied that a fraction of Dox was physically trapped by the unmodified SNPs. Compared to free Dox and Dox with unmodified SNPs, Dox loaded with oxidized SNPs showed a slower and sustained release profile. These results also indicated that Dox was successfully loaded into the oxidized SNPs. If the drugs were not loaded, a rapid release profile of free drugs would be observed. Free drugs can diffuse rapidly through the dialysis membrane.

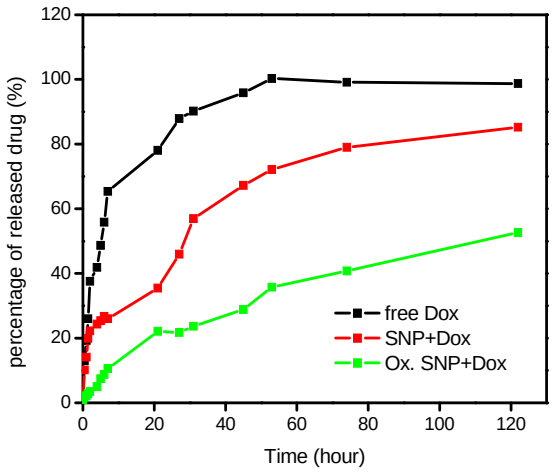

Figure 24. The release profiles of free Dox and Dox adsorbed by unmodified SNPs and oxidized SNPs.

Since weakly acidic environments are found endosomal and lysosomal compartments of tumor cells,[128] Dox release profiles were monitored in both biologically neutral and acidic condition. Compared to a biologically neutral environment at pH 7.4, a faster release profile was observed in a tumor tissue environment at pH 5 as shown in Figure 25. These phenomena are consistent with previous studies about Dox release at different pHs.[129–131] The reason for the faster release of Dox at pH 5 is that carboxylate anions on oxidized SNPs can be partially protonated under acidic conditions. Consequently, the electrostatic interactions between Dox and oxidized SNP are weakened, leading to more Dox being released.

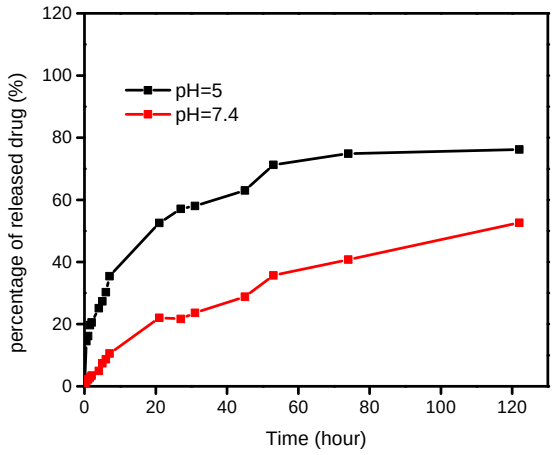

Figure 25. Effect of pH on Dox release profiles in oxdized SNPs.

3.4.4 Toxicity of the conjugate

After loading Dox onto oxidized SNPs, the toxicity of the drug conjugate was tested via incubation with HeLa cells. The MTT assay was performed to compare the toxicity of the vehicles, the free drug and the drug conjugate. Figure 26A shows that the oxidized SNPs are almost non-toxic as drug delivery vehicles, while drug conjugates kill cancer cells effectively in a certain concentration range. In Figure 26B, the efficacy of the drug conjugate is similar to that of the free Dox.

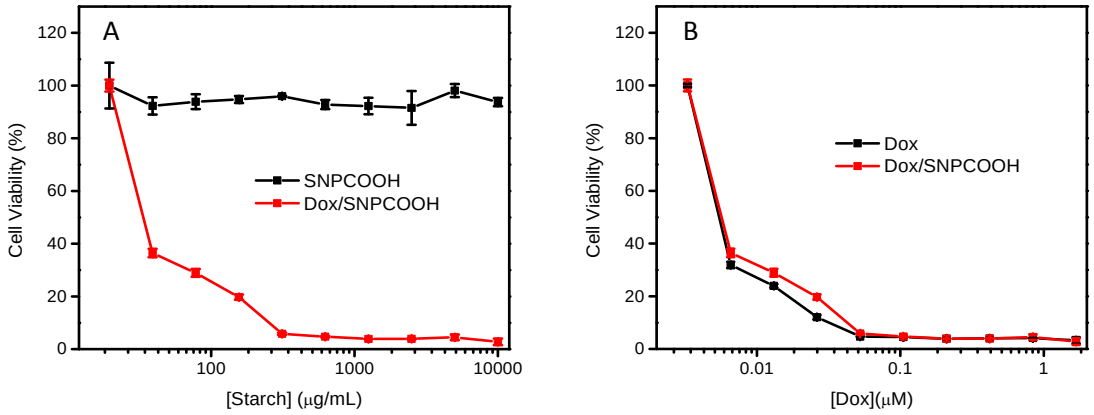

Figure 26. Comparison of toxicity of Dox/SNPs complexes with that of A) free oxidized SNPs and B) free Dox.

3.5 Summary and future work

This chapter reported the synthesis and characterization of carboxyl-modified SNPs and its capacity for drug loading. Doxorubicin was used as a model drug for the delivery study. Due to the positive charge of Dox, SNPs were functionalized with negatively charged carboxylate groups by TEMPO oxidation. The oxidation levels of SNPs were characterized by UV-vis absorption. The adsorption of Dox onto the oxidized SNPs was monitored by the fluorescence quenching of Dox. The adsorption titration experiments indicated that oxidized SNPs with carboxylate groups can strongly adsorb cationic Dox by electrostatic interactions, while the non-oxidized SNPs can only physically trap Dox in their the gel-like structures. After Dox was loaded onto the SNPs, the efficacy of the drug conjugate was tested and compared to that of free Dox. A cell viability study demonstrated the comparable toxicity of the Dox/SNP complexes and free Dox. Meanwhile, sustained and slow release profiles of Dox were achieved in both biologically neutral and acidic environments.

Since the level of crosslinking is partly responsible for the porosity of SNPs, which can be used to control the release rate, the effect of crosslinking densities on Dox release profiles should be studied in the future. Salt concentration also plays an important role in drug diffusion; therefore, the effect of salt in drug release profiles also needs to be tested. Due to the lack of time, the drug release profiles were not carried out in triplicate. The effect of oxidation levels of the SNPs on drug loading also can be investigated. Additionally, the quenched fluorescence intensities of Dox varied with time and pH, which made it hard to quantify the adsorption capacity of the oxidized SNPs for Dox. If reagents can be found to recover the quenched fluorescence of Dox, the drug loading capacity could be quantified in future work. To further understand the mechanism of fluorescence quenching between Dox and SNPs, fluorescence lifetime measurement can be performed in the future.

3.6 Materials and methods

3.6.1 Materials

SNPs were supplied by EcoSynthetix Inc. (Burlington, ON, Canada). Dox, MTT, TEMPO, NaBr and 5% bleach were purchased from Sigma-Aldrich (St Louis, MO, US). HEPES, citrate acid and their sodium salt were from Mandel Scientific (Guelph, ON, Canada). Dialysis tube (cut-off = 5 kDa) was purchased from Spectrum Laboratories (Rancho Dominguez, CA). Aqueous solutions were prepared using Milli-Q water (18.2 MΩ resistivity).

3.6.2 TEMPO oxidation and characterization

5% (w/w) SNPs solution was prepared by dispersing 5 g of SNPs into 100 mL Milli-Q water at 80 °C. These were subject to TEMPO oxidation using methods discussed in the literature.[36] 5% w/w SNPs were slowly stirred with 47.5 mg TEMPO and 635 mg NaBr in Milli-

Q water. Then 13 mL of 5% NaClO (bleach) was added to oxidized SNPs gradually. The pH of the solution should be maintained around 10.75 by adding 0.5 M NaOH for the reaction to proceed. The gradual addition process of bleach and NaOH was described in section 2.5.2. The reaction was quenched by adding 300 mL ethanol. Oxidized SNPs were precipitated out in ethanol. The precipitate was washed, centrifuged, and then lyophilized to form a white powder. Different oxidation levels of SNPs (1, 2, 5, 10, and 20%) were synthesized via adjusting the NaOH and bleach added. UV-vis spectroscopy was carried out for SNPs with different oxidation levels using an Agilent 8453 spectrophotometer. The SNPs samples with different oxidation levels used in UV-vis spectroscopy were papered in HEPES (pH 7.5) at a concentration of 0.1 mg/mL.

3.6.3 Drug loading and release

The SNPs were fully dispersed to 5% (w/w) in PBS (pH 7.4) and citrate acid (pH 5), respectively. Next, doxorubicin·HCl (Dox) was added to constitute 5% of the mass of SNPs. The Dox loaded SNPs (unmodified SNPs and oxidized SNPs) containing 5% Dox were dispersed in water at a concentration of 3 mg/mL and loaded in a dialysis tube Float-A-Lyzer® G2 from Spectrum Laboratories with MW cutoff at 5 kDa. This sample was then placed in a vial containing 35 mL of PBS or citrate acid with constant magnetic stirring and then allowed to sit for 120 hours at 36 °C. 400 µL samples were drawn off at 0, 0.5, 1, 2, 3, 4, 6, 10, 20, 24, 36, 48, 52, 78 and 120 hours. The fluorescence spectra of 400 µL samples were collected using a Varian Cary Eclipse fluorescence spectrometer at room temperature. The excitation wavelength was set at 485 nm and then the emission peaks were scanned from 500 to 700 nm.

3.6.4 Cytotoxicity study of drug conjugate

Cell culture and MTT assay. The toxicity study of the drug conjugate was performed using the same procedure described in Section 2.5.3. The only difference was the freshly prepared culture medium containing free Dox, free oxidized SNPs and SNP/Dox conjugates at the desired concentration.

Chapter 4 Cationic SNPs for gene delivery

4.1 Introduction

In this chapter, cationic SNPs were employed as vehicles for DNA delivery. Current gene delivery vehicles are mostly based on cationic polymers and cationic liposomes. While examples of inorganic nanoparticle-based delivery methods are also reported, their difficulty to degrade may pose safety concern. As SNPs are biodegradable and should have excellent biocompatibility, they are expected to be good candidates for gene delivery vehicles. However, the unmodified SNPs do not interact with DNA strongly. A logic method to increase DNA affinity is via cationic modification of SNPs. The size and surface charge of the cationic SNPs developed by my co-worker Duncan Li were evaluated in this chapter. Meanwhile, the safe concentration range of the cationic SNPs used for gene delivery was determined by cell viability study. In order to balance the safety and efficiency of the gene delivery system, the ratios of cationic SNPs and DNA employed were carefully evaluated by gel retardation assay. Finally, the DNA complexes was delivered to HeLa cells with efficiency comparable to that of a commercial transfection reagent, Lipofectamine.

4.2 Synthesis of cationic SNPs and characterization

To synthesize cationic SNPs, my co-worker Duncan Li took the unmodified SNPs and introduced a cationic quaternary ammonium group onto the backbone of SNPs. Although starch has been modified with several types of cationic groups such as phosphonium and sulfonium groups, by far the most common approaches for cationic starch modifications are via introducing ammonium groups such as 3-chloro-2-hydroxypropyltrialkylammonium chlorides (CHPTMA).[93] As described in the reaction scheme presented in Figure 27, cationic SNPs were synthesized by

grafting CHPTMA onto SNPs under basic conditions. The degree of substitution for the cationic SNPs was determined by ^{1}H-NMR.

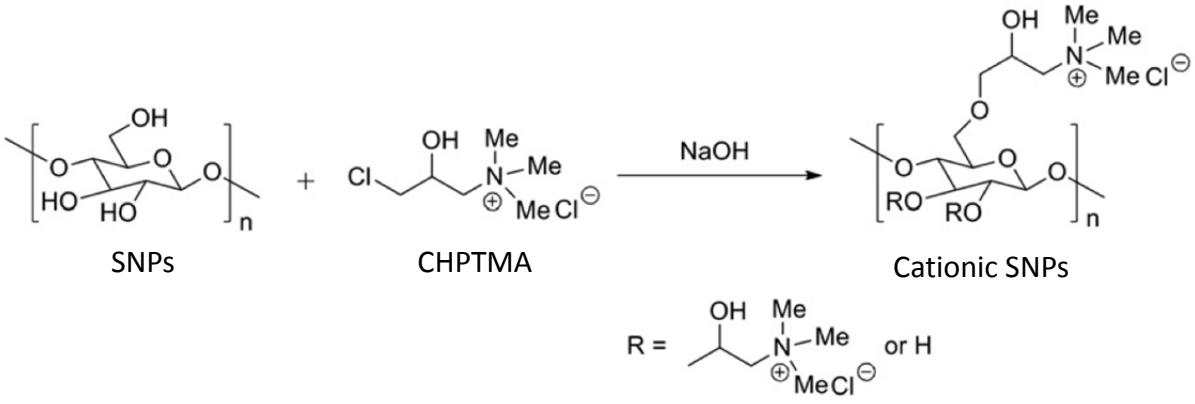

Figure 27. Synthesis process of cationic SNPs by introducing the cationic CHPTMA.

To characterize the size of the cationically modified SNPs, DLS was employed to measure the hydrodynamic diameters of the cationic SNPs. Three types of cationic SNPs with different degrees of substitution (0.17, 0.24, 0.35) were dissolved in Milli-Q water and DMSO, respectively. The size distributions of the SNPs are similar in water and DMSO as shown in Figures 28A and 28B. According to the number based size distribution, 99.9% of the cationic SNPs were found to be between 9 to 30 nm depending on the degree of substitution. The size of the cationic SNPs is smaller than the unmodified SNPs, suggesting that degradation of the SNPs takes place during the cationic modification.

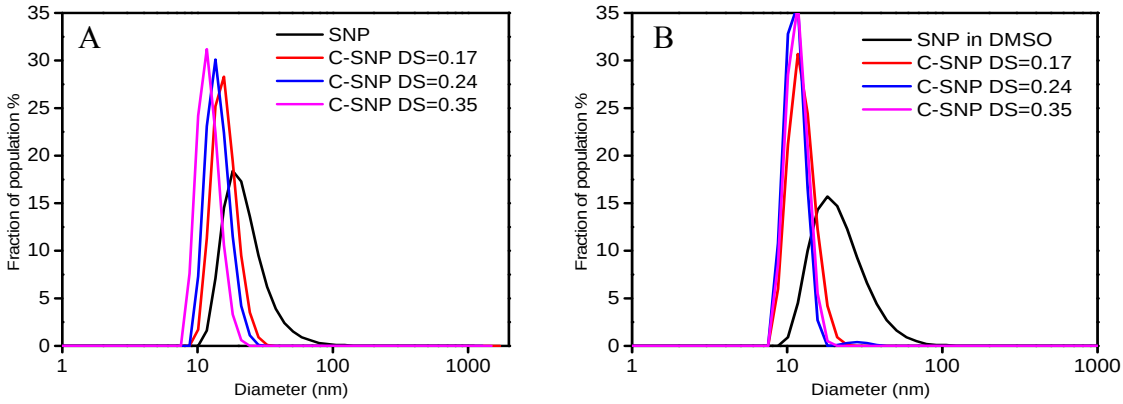

Figure 28 The number based size distribution of cationic SNPs in A) water and B) DMSO.

To characterize the surface charge, the ζ-potentials of the cationic SNPs were measured. Compared with the unmodified SNPs, all of the cationic SNPs have positive surface charges as shown in Figure 29. With the degree of substitution increasing from 0.17 to 0.35, the ζ-potential of the cationic SNPs increased from 20 to 30 mV. These ζ-potential results demonstrated that the SNPs were successfully modified with positive surface charges. Meanwhile, the surface charge of the cationic SNPs increased with increasing degree of substitution.

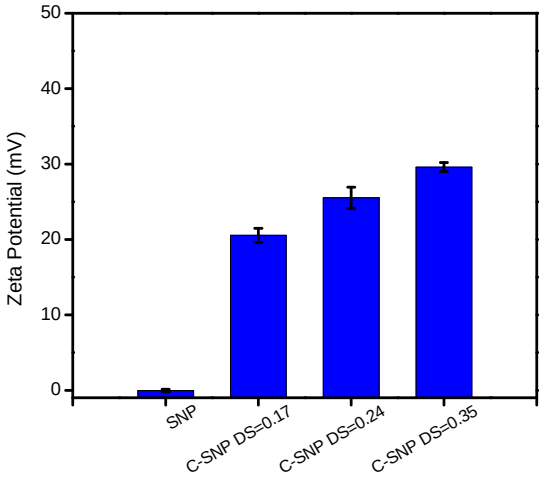

Figure 29 ζ-potentials of cationic SNPs with different degrees of substitution.

4.3 Toxicity of cationic starch nanoparticles

Since we used cationic SNPs as vehicles for gene delivery, it is necessary to evaluate their cytotoxicity. Cationic SNPs, unmodified SNPs, and other commercial cationic reagents were incubated with HeLa cells to compare the cytotoxicity of these reagents. The MTT assay was conducted to measure cell viability and the results are summarized in Figure 30. Unmodified SNPs do not induce cell death when the concentration is lower than 10 mg/mL. However, 0.1 mg/mL of cationic SNPs can cause 40% cell death. Similar toxicity can be observed for cationic SNPs with different degrees of substitution. In conclusion, no obvious trend can be observed between the toxicity and the degrees of substitution. All cationic SNPs are more toxic than unmodified SNPs as shown in Figure 30A. The reason is that most of the cell membranes have negative surface charges and cationic nanoparticles can penetrate into the cell membranes more easily causing damage to the cell membrane. As a result, particles with cationic charges are considered to be more toxic than neutrally or negatively charged particles.

In order to compare the toxicity of cationic SNPs with other commercial transfection agents, cationic liposomes (lipofectamine, DOTAP) and cationic polymers (PEI) were also selected for incubation with HeLa cells. The concentrations of SNPs and other gene transfection agents were adjusted to achieve the same N/P ratio when used for complexation with DNA. N/P ratio is the molar ratio between positive nitrogen groups of cationic reagents and negative phosphate groups on the DNA backbone. As shown in Figure 30B, cells treated with the cationic SNPs can achieve 82% viability; while Lipofectamine, DOTAP, PEI result in 79%, 69% and 58% cell viability, respectively. These results indicated that the toxicity of cationic SNPs was slightly lower than other cationic agents at the same N/P ratio.

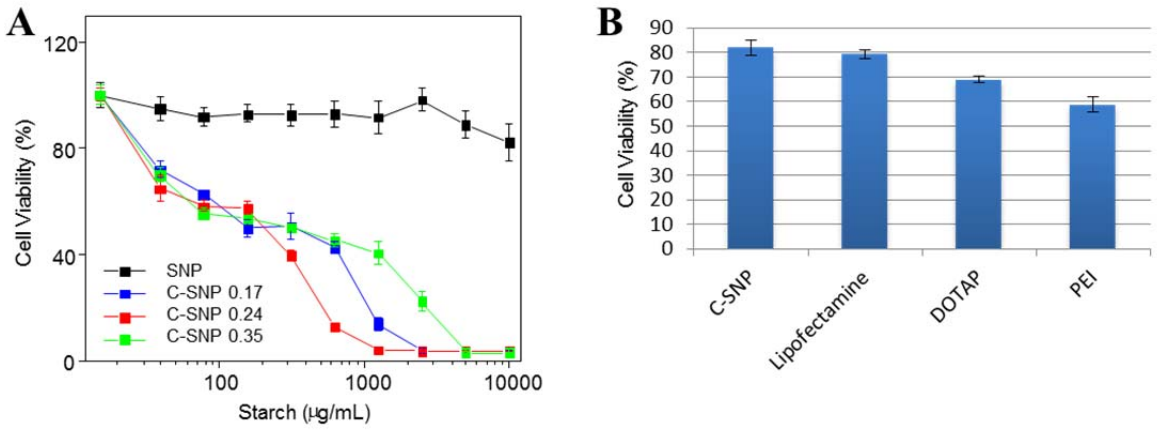

Figure 30. A) Toxicity of cationic SNPs with different degrees of substitution and B) Toxicity of cationic SNPs and other commercial cationic reagents at the same N/P ratio.

4.4 DNA loading and release

4.4.1 DNA binding property

To further understand the binding property between DNA and cationic SNPs, we performed agarose gel electrophoresis experiments. Cationic SNP/DNA complexes formation is based on electrostatic interactions between the positive charges of cationic SNPs and the negative charges of DNA. The concentration of DNA was fixed; cationic SNPs were added to DNA to form cationic SNP/DNA complexes at various N/P molar ratios.

In the gel image shown in Figure 31A, lane one is the free FAM-labeled DNA, which migrates towards the positive electrode as a strong band. With the concentration of cationic SNPs increasing, the bands are more retarded and show more smearing. All of the DNA is trapped in the well when the N/P ratio is reached 2.0, indicating DNA is adsorbed onto the cationic SNPs. It is worthy of note that if DNA is not adsorbed onto the cationic SNPs, the free DNA is supposed to migrate the same distance and run to the same position as shown in the case of DOTAP in Figure 31B. However, in the case of the cationic SNPs, the small size cationic

SNPs can migrate with DNA in the gel. With the concentration of the cationic SNPs increasing, the SNPs can associate with more DNA and trap the DNA in the well once the negative charges of DNA are neutralized by the cationic SNPs via electrostatic attractions. As shown in Figure 32, many DNA are adsorbed on the surface of the same SNPs at low N/P ratio. As a result, the negative charges of DNA are not completely neutralized by association with the cationic SNPs at low N/P ratio, resulting in the SNP/DNA complexes having a net negative charge. Due to the negative charge of SNP/DNA complexes, the cationic SNPs with a small size can migrate with DNA under the electric field. With the N/P ratio increasing, more positive charges of the cationic SNPs are available to interact with DNA. Meanwhile, the number of DNA adsorbed on the surface of each cationic SNPs is decreased as shown in Figure 32. As a result, the negative charge of cationic SNP/DNA complexes is neutralized. The mobility of the cationic SNP/DNA complexes is reduced. Finally, all of DNA is adsorbed by the cationic SNPs and the charge of cationic SNP/DNA complexes becomes neutral or positive, resulting in all the DNA complexes being trapped in the well.

To confirm the above hypothesis, the interaction between cationic liposomes DOTAP with DNA was monitored as control groups. DOTAP is a cationic lipid that forms liposome with stable size range from 120 to 140 nm, which is not able to migrate in the gel. As shown in Figure 31B, free DNA migrates to the same position as expected. With the N/P ratio increasing from 0.125 to 4, more positive charges of the cationic liposomes are available to interact with DNA. Therefore, the amount of free DNA is decreased, resulting in less bright bands of free DNA. Meanwhile, the amount of DNA trapped by DOTAP liposomes increases inside the wells. In conclusion, gel electrophoresis experiments have confirmed the small size of SNPs; yet the cationic SNP/DNA complexes was stable enough to survive gel electrophoresis. Meanwhile, we

determined that two was the minimal N/P ratio for full complexation with DNA by gel retardation experiments.

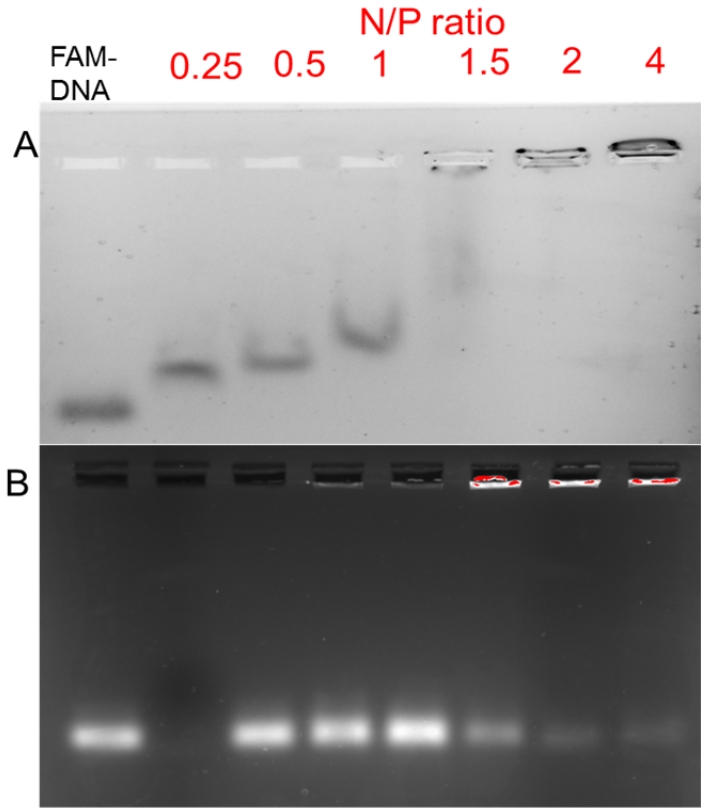

Figure 31 Gel image of the DNA interaction with A) cationic SNP, B) DOTAP.

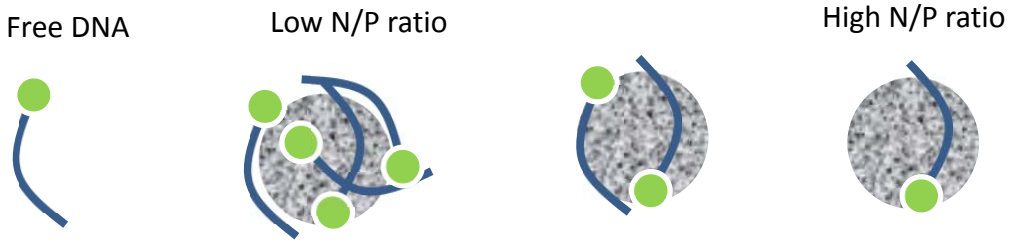

Figure 32. Interaction between DNA and cationic SNPs at different N/P ratios.

4.4.2 Deliver DNA to cancer cells

To compare the cell internalization efficiency of cationic SNPs with that of a commercial gene transfection agent, Lipofectamine, we examined the cellular uptake by laser scanning

confocal fluorescence microscopy after incubating DNA complexes with cancer cells. The confocal images of the cationic SNP/DNA, lipofectamine/DNA, and free DNA are shown in Figure 33. DNA was labeled with FAM shown in green. The nucleus areas were stained with blue. Cell borders were stained with yellow. The free DNA as the negative control group cannot cross the cell membrane. The cationic SNP/DNA complexes can go through the membrane and reaching the nucleus, achieving an internalization effect comparable to that observed with the commercial gene transfection agent, Lipofectamine.

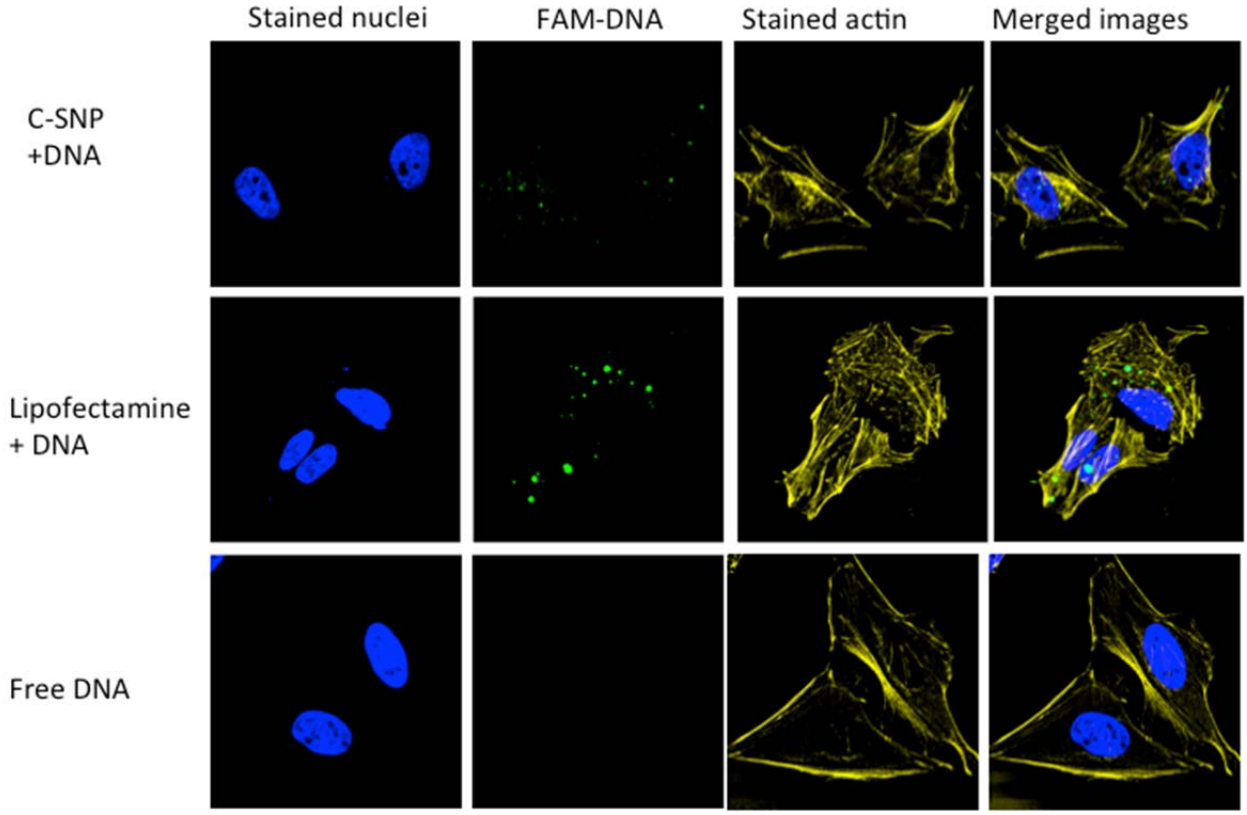

Figure 33. Cellular uptake images of cationic SNP/DNA complexes, lipofectamine/DNA complexes, and free DNA.

4.5 Summary and future Work

This chapter reported the preparation and characterization of the cationic SNPs and their interactions with DNA. The cationic SNP/DNA complexes were delivered to cells with an efficiency comparable to that of a commercial gene transfer agent, Lipofectamine. The cationic SNPs were synthesized by my co-worker Duncan Li through the introduction of cationic quaternary ammonium groups onto the SNP backbone. After cationic modification, the cationic SNPs had a hydrodynamic diameter (D_h) around 10 nm with positive surface charge. Meanwhile, the cationic SNPs with a higher degree of substitution had a higher positive surface charge. In cytotoxicity study, the cationic SNPs showed lower toxicity than other commercially available gene transfection agents. After DNA was bound to the cationic SNPs by electrostatic interactions, the binding property was investigated by gel electrophoresis at different N/P molar ratios. We determined a the N/P ratio of 2.0 was the minimal ratio resulting in full complexation of the cationic SNPs with DNA. Furthermore, the successful DNA transfection was observed and the transfection efficiency was comparable to that of Lipofectamine, a commercial gene transfection agent. These results demonstrated the biocompatible potential of the cationic SNPs as a gene delivery platform.

After binding DNA onto the cationic SNPs, the size and surface charge of the DNA/SNPs complexes should be measured. Since the mobility of sample loaded in gel depends on the size and charge of the sample, these measurements can help understand the results of gel retardation experiments. The gel retardation experiments also can be conducted using polyacrylamide gel due to its better resolution. The amount of DNA internalized by cell can be quantified using flow cytometry in the future.

4.6 Materials and methods

4.6.1 Materials

All SNPs were provided by EcoSynthetix Inc. (Burlington, ON, Canada). The cationic SNPs were synthesized by Duncan Li in Dr. Scott Taylor's group at the University of Waterloo. DNA samples were purchased from Integrated DNA Technologies (IDT, Coralville, IA). The FAM-labeled 24-mer DNA sequence is FAM-ACGCATCTGTGAAGAGAACCTGGG. DOTAP was purchased from Avanti Polar Lipids (Alabaster, AL). Lipofectamine 2000 was purchased from Invitrogen. HEPES and DMSO were purchased from Mandel Scientific Inc. (Guelph, ON, Canada). HeLa cell line (CCL-2^{TM}) was obtained from the American Type Culture Collection (ATCC, Manassas, Virginia) through the help of the laboratory of Dr. Shirley Tang (Waterloo, Ontario). MTT was purchased from Sigma-Aldrich (St Louis, MO). Agarose powder (50004) was purchased from Ornat. All the buffers and solutions were prepared with Milli-Q water.

4.6.2 Dynamic light scattering (DLS) and ζ-potential measurements

To obtain pH-dependent size and ζ-potential, cationic SNPs with different degrees of substitution (1 mg/mL) were dispersed in designed 5 mM HEPES buffer solutions (pH 7.5). The hydrodynamic sizes of SNPs were measured using a dynamic light scattering (Zetasizer Nano 90, Malvern). The reported size was the average diameter (number based) of three runs. Each run consisted of ten measurements for 1 min each. The same samples were used for ζ-potential measurement on a Malvern Zetasizer Nano ZS90 at 90° collecting optics. Averages of three runs were made. The data were analyzed by Malvern Dispersion Technology Software 4.20.

4.6.3 Cytotoxicity study of cationic SNPs

Cell culture and MTT assay. The toxicity study of the conjugate was performed using the same procedure described in Section 2.5.3. The only difference was the freshly prepared culture medium containing cationic SNPs with different degrees of substitution (0.17, 0.24, 0.36) at the desired concentration. The concentration of SNPs and other gene transfection agents were adjusted by achieving a same N/P ratio with DNA. The concentrations of cationic SNP, lipofectamine, DOTAP, and PEI were 20 μg/mL, 1μL/20 μL, 100μg/mL and 25 μg/mL, respectively.

4.6.4 Preparation of cationic SNP/DNA and liposome/DNA complexes

Agarose gel electrophoresis. The binding between cationic SNPs and FAM-DNA was investigated by agarose gel electrophoresis. The complexes of cationic SNP, DOTAP and FAM-DNA were prepared at various N/P molar ratios (0.25, 0.5, 1, 1.5, 2, 4). The concentration of FAM-DNA was fixed at 100 nM. The concentrations of cationic SNPs and liposomes were tuned according to the required N/P ratio. Free FAM-DNA (100 nM) was also included for comparison. The gel was prepared with 2% agarose and 1× TBE (pH 7). 40 μL of DNA-cationic SNP/liposome conjugates containing 50% glycerol were added to each lane. The gel was run at 120 V for 40 mins. The running buffer is 1× TBE (pH 7). The FAM-DNA bands were imaged using a gel documentation system (Chemidoc-MP, Bio-Rad).

Preparation of liposomes. 1) Preparation of lipids film: 2.5 mg of DOTAP lipids were dissolved in chloroform. Then chloroform was evaporated to form a lipid film using gentle a N_2 flow. The lipid film was further dried to remove the residual chloroform by placing the samples in a vacuum oven overnight. The dried lipid film was kept under N_2 and the container was taped tightly and stored at -20 °C until ready to hydrate. 2) Hydration of lipid film: The hydration of

the dry DOTAP film was performed by adding 0.5 mL buffer A (100 mM NaCl, 10 mM HEPES, pH 7.6) to the container at room temperature. Finally, the concentration of lipid was 5 mg/mL. Then the suspension was occasional sonicated for 2 h to form a cloudy suspension. 3) Sizing of lipid suspension: the DOTAP liposomes were prepared using the standard extrusion process. A mini-extruder from Avanti was used to maintain the mean diameter of DOTAP liposome around 120-140 nm. The resulting cloudy suspension was forced through two stacked polycarbonate filter membrane (pore size =100 nm) for 21 times to downsize the lipid dispersion. After extrusion, the transparent lipid solution suggested the formation of liposomes.

4.6.5 Cellular uptake of cationic SNP/DNA complexes

Laser scanning confocal fluorescence microscopy. Cellular uptake of cationic SNP/DNA complexes was visualized using a confocal microscope. HeLa cells were seeded onto 14 mm coverslips in 24-well plates at a density of 50,000 cells per well. 500 μL of cell medium was added to culture cells and allowed to grow to ~60% confluency. In the cellular uptake experiment, the cells were incubated with cationic SNP/DNA, lipofectamine/DNA, and free DNA at N/P ratio two for 3 h at 37 °C. The concentration of DNA was fixed at 200 nM. The concentrations of cationic SNPs and liposome were tuned according to the N/P ratio. After the designated incubation time 2h, the cells were washed twice with PBS buffer and fixed by 4% paraformaldehyde (in PBS buffer) for 15 min at room temperature. The cells were further washed three times with PBS. Then the cell actin was stained with Alexa Fluor 488 phalloidin and the cell nuclei were stained with DAPI by the incubation for 5 min according to the manufacturer's procedures. Images of cells were captured using DAPI and Alexa Fluor 488 channels under a laser scanning confocal fluorescence microscope (LSM510Meta, CarlZeiss Inc., Thornwood, NY).

Chapter 5 Conclusions and recommendations

5.1 Conclusions

This thesis began with an overview of the advantages of nanocarriers and an introduction of nanomaterials applied as drug and gene delivery vehicles. After a literature review about the applications of different nanomaterials in drug delivery systems, SNPs were proposed to be good candidates for drug delivery due to their good biocompatibility. The chemical structure and properties of starch and SNPs were discussed. Different preparation methods and chemical modifications of SNPs were then presented. After reviewing the relevant work related to the use of SNPs as nanocarriers, we explored the applicability of the modified SNPs for drug and gene delivery. With this in mind, this thesis was divided into the three following sections: 1) The study of the toxicity of SNPs supplied by EcoSynthetix and the development of a method to eliminate their toxicity; 2) the synthesis and characterization of carboxylated SNPs for Dox delivery; and 3) the characterization of cationically modified SNPs for delivering DNA into cancer cells. These objectives sought to establish SNPs as a new platform for drug and gene delivery. An overview of the conclusions reached in this thesis is provided hereafter.

Glyoxal used as a crosslinking agent in the preparation of SNPs was found to be at the origin of the toxicity of the SNPs. The toxicity of the SNPs is believed to result from the reaction of glyoxal with the amino groups of proteins, nucleotides, and lipids. The products of these reactions appear to cause cell damage. The toxicity of the unmodified SNPs increased with increasing crosslinker density. In an interesting experiment, the GX0 sample spiked with an amount of glyxoal similar to that used by Ecosynthetix to prepare the GX5 sample had a similar toxicity as that of the GX5 SNP. These results demonstrated that unbound glyoxal is the source

of the toxicity of the SNPs. Fortunately, these free glyoxal molecules can be removed by washing the SNPs with ethanol resulting in glyoxal-free SNPs that were almost non-toxic.

SNPs were also carboxylated by TEMPO oxidation. The oxidation of starch mediated by TEMPO can selectively oxidize the primary hydroxyls of the SNPs into carboxyl acids. The oxidation level of the SNPs was characterized by UV-vis absorption. The size and surface charge of the SNPs with different oxidation levels were also determined. The positively charged Doxorubicin (Dox) was used as a model drug and it could bind strongly onto the oxidized SNPs by electrostatic interactions. The orange fluorescence of Dox was quenched by the addition of the oxidized SNPs. As a result, fluorescence quenching of Dox was employed to characterize its binding onto the carboxylated SNPs. Titration of Dox with the oxidized SNPs and the unmodified SNPs demonstrated strong binding of Dox onto the oxidized SNPs by electrostatic interactions. Residual binding of Dox onto the unmodified SNPs was attributed to physical trapping of Dox in the gel-like structure of the SNPs. By comparing the drug release profiles of Dox loaded onto the oxidized SNPs with that of free Dox and Dox bound to the unmodified SNPs, a sustained and slow release profile of Dox loaded onto the oxidized SNPs was observed in both biologically neutral and acidic conditions. After incubating the Dox/SNPs complexes with HeLa cells, the drug complexes could kill the cells effectively.

Cationic SNPs were also investigated in this thesis. The cationic SNPs were modified with cationic quaternary ammonium groups. The size and surface charge of the cationic SNPs were characterized. The cationic SNPs had a hydrodynamic diameter (D_h) around 10 nm in DMSO and water. Comparison of the D_h values obtained with the modified and unmodified SNPs led to the conclusion that the cationic SNPs were smaller, indicating some level of degradation during the cationic modification. Three cationic SNPs with different degrees of

substitution were investigated. All modified SNPs showed a positive surface charge with the SNPs having a higher degree of substitution yielding higher surface charges. These results based on ζ-potential measurements demonstrated successful cationic modification of the SNPs. The toxicity of the modified SNPs was evaluated by using different SNP concentrations in the MTT assay. The result provided a safe concentration range where the cationic SNPs could be applied to gene delivery. In comparison with other commercially available cationic agents, the toxicity of the cationic SNPs was found to be slightly lower. The DNA binding process was investigated by gel retardation experiments. These experiments led to the conclusion that a N/P ratio of 2.0 was the minimal ratio to yield full complexation of the cationic SNPs with DNA. After binding DNA onto the cationic SNPs by electrostatic interactions, cellular uptake of the DNA/SNPs complexes was achieved and the uptake efficiency was comparable to that of Lipofectamine, a commercial gene transfection agent.

5.2 Recommendations for future work

The results described in this thesis lead to a number of recommendations for the development of SNPs as nanocarriers for drug and gene delivery. These recommendations are summarized as follows: 1) Enhancement of the biocompatibility of the unmodified SNPs; 2) enhancement of the efficacy of the delivery systems; 3) immune response test for the drug complexes; 4) evaluation of the therapeutic effect of the complexes *in vivo*.

1) Enhancement of the biocompatibility of the unmodified SNPs

Since the free glyoxal molecules are responsible for the toxicity of the SNPs, the origin of the free glyoxal should be studied in the future. There are two possible sources: 1) some glyoxal

molecules are not involved in the crosslinking process during the manufacturing of the SNPs; 2) some glyoxal molecules are released from the SNPs when dispersed in water due to the reversible crosslinking reaction. The inherent toxicity of glyoxal mandates that other biocompatible and stable crosslinking agents such as sodium trimetaphosphate (STMP) be investigated to crosslink the SNPs instead of glyoxal.

2) Enhancement of the efficacy of the delivery systems

Some clinical studies have shown that the incorporation of more than one anti-cancer drug can enhance anticancer efficiency by a synergistic effect.[36] Most reported polysaccharide platforms are based on Dox delivery, but the work on cisplatin is limited. Cisplatin, as another common anticancer drug, also has a number of problems such as low solubility and cardiotoxicity. Since Dox and cisplatin have drastically different chemical structures, properties, and efficacy, multiple drugs could be loaded to the SNPs and delivered to improve their anti-cancer efficacy. However, different drugs might compete for the surface binding sites on the SNPs when co-delivered. Subsequent studies about co-delivery of cisplatin and Dox can be explored in the future. It is expected that co-delivery of cisplatin and Dox would suppress cancer growth more efficiently than individual drugs.

Since small interfering RNA (siRNA) and micro RNA (miRNA) can induce gene silencing by targeting specific genes, their delivery and inhibition effect on gene expression can be performed by cationic SNPs. Subsequent studies on the function of nucleic acids in terms of the suppression of gene expression can be further explored. The co-delivery of gene and small molecular drugs such as Dox and cisplatin are also worth exploring in future work. Currently, common gene delivery vehicles are expensive and may pose safety concern, depending on their

chemical structures. The cationic SNPs might be a cost-effective method to improve gene transfection efficacy.

3) Immune response test for the drug complexes

Drug complexes are foreign to the body, and as such, can be recognized by the immune system and activate the immune response when circulating in the bloodstream. Phagocytic cells participating in inflammation represent a major part of the body's immune mechanism.[132] Therefore, the immune response of macrophages treated with drug complexes should be evaluated in future work.

4) Evaluation of the therapeutic effect of the complexes *in vivo*

After promising drug/SNP complexes are recognized, it should be examined with *in vivo* experiments using animal models bearing tumors. However, the cost of an *in vivo* study is much higher than that of an *in vitro* study. Therefore, the drug/SNP complexes should be optimized to have the best stability and biocompatibility. Different cancer cell lines should also be tested for this drug delivery system.

References

(1) Jemal, A.; Bray, F.; Center, M. M.; Ferlay, J.; Ward, E.; Forman, D. Global Cancer Statistics. *CA. Cancer J. Clin.* **2011**, *61*, 69–90.

(2) Cancer Facts & Figures 2015. *Am. Cancer Soc. Inc* **2015**, 1.

(3) Helleday, T.; Petermann, E.; Lundin, C.; Hodgson, B.; Sharma, R. A. DNA Repair Pathways as Targets for Cancer Therapy. *Nat. Rev. Cancer* **2008**, *8*, 193–204.

(4) Wang, A. Z.; Langer, R. S.; Farokhzad, O. C. Nanoparticle Delivery of Cancer Drugs. *Annu. Med* **2012**, *63*, 185–198.

(5) Peer, D.; Karp, J. M.; Hong, S.; Farokhzad, O. C.; Margalit, R.; Langer, R. Nanocarriers as an Emerging Platform for Cancer Therapy. *Nat. Nano* **2007**, *2*, 751–760.

(6) Davis, M. E.; Chen, Z. (Georgia); Shin, D. M. Nanoparticle Therapeutics: An Emerging Treatment Modality for Cancer. *Nat. Rev. Drug Discov.* **2008**, *7*, 771–782.

(7) Arap, W.; Haedicke, W.; Bernasconi, M.; Kain, R.; Rajotte, D.; Krajewski, S.; Ellerby, H. M.; Bredesen, D. E.; Pasqualini, R.; Ruoslahti, E. Targeting the Prostate for Destruction through a Vascular Address. *Proc. Natl. Acad. Sci.* **2002**, *99*, 1527–1531.

(8) Dausend, J.; Musyanovych, A.; Dass, M.; Walther, P.; Schrezenmeier, H.; Landfester, K.; Mailänder, V. Uptake Mechanism of Oppositely Charged Fluorescent Nanoparticles in HeLa Cells. *Macromol. Biosci.* **2008**, *8*, 1135–1143.

(9) Ruoslahti, E. Peptides as Targeting Elements and Tissue Penetration Devices for Nanoparticles. *Adv. Mater.* **2012**, *24*, 3747–3756.

(10) Guzmán, K. A. D.; Taylor, M. R.; Banfield, J. F. Environmental Risks of Nanotechnology: National Nanotechnology Initiative Funding, 2000-2004. *Environ. Sci. Technol.* **2006**, *40*, 1401–1407.

(11) Nakagawa, Y.; Wakuri, S.; Sakamoto, K.; Tanaka, N. The Photogenotoxicity of Titanium Dioxide Particles. *Mutat. Res.* **1997**, *394*, 125–132.

(12) Shvedova, A. A.; Castranova, V.; Kisin, E. R.; Schwegler-Berry, D.; Murray, A. R.; Gandelsman, V. Z.; Maynard, A.; Baron, P. Exposure to Carbon Nanotube Material: Assessment of Nanotube Cytotoxicity Using Human Keratinocyte Cells. *J. Toxicol. Environ. Health. A* **2003**, *66*, 1909–1926.

(13) Lam, C.-W.; James, J. T.; McCluskey, R.; Hunter, R. L. Pulmonary Toxicity of Single-Wall Carbon Nanotubes in Mice 7 and 90 Days after Intratracheal Instillation. *Toxicol. Sci.* **2004**, *77*, 126–134.

(14) Warheit, D. B.; Laurence, B. R.; Reed, K. L.; Roach, D. H.; Reynolds, G. A. M.; Webb, T. R. Comparative Pulmonary Toxicity Assessment of Single-Wall Carbon Nanotubes in Rats. *Toxicol. Sci.* **2004**, *77*, 117–125.

(15) Silverman, J. A.; Deitcher, S. R. Marqibo® (vincristine Sulfate Liposome Injection) Improves the Pharmacokinetics and Pharmacodynamics of Vincristine. *Cancer Chemother. Pharmacol.* **2013**, *71*, 555–564.

(16) Kolishetti, N.; Dhar, S.; Valencia, P. M.; Lin, L. Q.; Karnik, R.; Lippard, S. J.; Langer, R.; Farokhzad, O. C. Engineering of Self-Assembled Nanoparticle Platform for Precisely Controlled Combination Drug Therapy. *Proc. Natl. Acad. Sci.* **2010**, *107*, 17939–17944.

(17) Kohli, A. G.; Kierstead, P. H.; Venditto, V. J.; Walsh, C. L.; Szoka, F. C. Designer Lipids for Drug Delivery: From Heads to Tails. *J. Control. Release* **2014**, *190*, 274–287.

(18) Barenholz, Y. Doxil®--the First FDA-Approved Nano-Drug: Lessons Learned. *J. Control. Release* **2012**, *160*, 117–134.

(19) Zalipsky, S.; Qazen, M.; Walker, J. A.; Mullah, N.; Quinn, Y. P.; Huang, S. K. New Detachable Poly(ethylene Glycol) Conjugates: Cysteine-Cleavable Lipopolymers Regenerating Natural Phospholipid, Diacyl Phosphatidylethanolamine. *Bioconjug. Chem.* **1999**, *10*, 703–707.

(20) Torchilin, V. P. Recent Advances with Liposomes as Pharmaceutical Carriers. *Nat. Rev. Drug Discov.* **2005**, *4*, 145–160.

(21) Duncan, R. The Dawning Era of Polymer Therapeutics. *Nat. Rev. Drug Discov.* **2003**, *2*, 347–360.

(22) Jarvan, C. M.; Gooderham, N. J.; Edwards, R. J.; Davies, D. S.; Shaunak, S. Anti-HIV Type 1 Activity of Sulfated Derivatives of Dextrin against Primary Viral Isolates of HIV Type 1 in Lymphocytes and Monocyte-Derived Macrophages. *AIDS Res. Hum. Retroviruses* **1997**, *13*, 875–880.

(23) Schrempf, W.; Ziemssen, T. Glatiramer Acetate: Mechanisms of Action in Multiple Sclerosis. *Autoimmun. Rev.* **2007**, *6*, 469–475.

(24) Bhadra, D.; Bhadra, S.; Jain, P.; Jain, N. K. Pegnology: A Review of PEG-Ylated Systems. *Pharmazie* **2002**, *57*, 5–29.

(25) Duncan, R. Polymer Therapeutics as Nanomedicines: New Perspectives. *Curr. Opin. Biotechnol.* **2011**, *22*, 492–501.

(26) Kim, T.-Y.; Kim, D.-W.; Chung, J.-Y.; Shin, S. G.; Kim, S.-C.; Heo, D. S.; Kim, N. K.; Bang, Y.-J. Phase I and Pharmacokinetic Study of Genexol-PM, a Cremophor-Free,

Polymeric Micelle-Formulated Paclitaxel, in Patients with Advanced Malignancies. *Clin. Cancer Res.* **2004**, *10*, 3708–3716.

(27) Lee, K.-W.; Kim, J. H.; Yun, T.; Song, E. K.; Na, I. il; Shin, H.; Oh, S. Y.; Choi, I. S.; Oh, D.-Y.; Kim, D.-W.; et al. Phase II Study of Low-Dose Paclitaxel and Cisplatin as a Second-Line Therapy after 5-Fluorouracil/Platinum Chemotherapy in Gastric Cancer. *J. Korean Med. Sci.* **2007**, *22*, S115–S121.

(28) Zhang, X.-Q.; Xu, X.; Lam, R.; Giljohann, D.; Ho, D.; Mirkin, C. A. Strategy for Increasing Drug Solubility and Efficacy through Covalent Attachment to Polyvalent DNA–Nanoparticle Conjugates. *ACS Nano* **2011**, *5*, 6962–6970.

(29) Gibson, J. D.; Khanal, B. P.; Zubarev, E. R. Paclitaxel-Functionalized Gold Nanoparticles. *J. Am. Chem. Soc.* **2007**, *129*, 11653–11661.

(30) Widder, K. J.; Senyei, A. E.; Scarpelli, D. G. Magnetic Microspheres: A Model System for Site Specific Drug Delivery in Vivo. *Exp. Biol. Med.* **1978**, *158*, 141–146.

(31) Lübbe, A. S.; Bergemann, C.; Riess, H.; Schriever, F.; Reichardt, P.; Possinger, K.; Matthias, M.; Dörken, B.; Herrmann, F.; Gürtler, R.; et al. Clinical Experiences with Magnetic Drug Targeting: A Phase I Study with 4′-Epidoxorubicin in 14 Patients with Advanced Solid Tumors. *Cancer Res.* **1996**, *56*, 4686–4693.

(32) Lübbe, A. S.; Bergemann, C.; Huhnt, W.; Fricke, T.; Riess, H.; Brock, J. W.; Huhn, D. Preclinical Experiences with Magnetic Drug Targeting: Tolerance and Efficacy. *Cancer Res.* **1996**, *56*, 4694–4701.

(33) Gang, J.; Park, S.-B.; Hyung, W.; Choi, E. H.; Wen, J.; Kim, H.-S.; Shul, Y.-G.; Haam, S.; Song, S. Y. Magnetic Poly E-Caprolactone Nanoparticles Containing Fe3O4 and Gemcitabine Enhance Anti-Tumor Effect in Pancreatic Cancer Xenograft Mouse Model. *J. Drug Target.* **2007**, *15*, 445–453.

(34) Yu, M. K.; Jeong, Y. Y.; Park, J.; Park, S.; Kim, J. W.; Min, J. J.; Kim, K.; Jon, S. Drug-Loaded Superparamagnetic Iron Oxide Nanoparticles for Combined Cancer Imaging and Therapy In Vivo. *Angew. Chem. Int. Ed.* **2008**, *47*, 5362–5365.

(35) Sheridan, C. Gene Therapy Finds Its Niche. *Nat. Biotechnol.* **2011**, *29*, 121–128.

(36) Mintzer, M. A.; Simanek, E. E. Nonviral Vectors for Gene Delivery. *Chem. Rev.* **2009**, *109*, 259–302.

(37) Jones, C. H.; Chen, C. K.; Ravikrishnan, A.; Rane, S.; Pfeifer, B. a. Overcoming Nonviral Gene Delivery Barriers: Perspective and Future. *Mol. Pharm.* **2013**, *10*, 4082–4098.

(38) Fraley, R. T.; Fornari, C. S.; Kaplan, S. Entrapment of a Bacterial Plasmid in Phospholipid Vesicles: Potential for Gene Transfer. *Proc. Natl. Acad. Sci.* **1979**, *76*, 3348–3352.

(39) Byk, G.; Dubertret, C.; Escriou, V.; Frederic, M.; Jaslin, G.; Rangara, R.; Pitard, B.; Crouzet, J.; Wils, P.; Schwartz, B.; et al. Synthesis, Activity, and Structure−Activity Relationship Studies of Novel Cationic Lipids for DNA Transfer. *J. Med. Chem.* **1998**, *41*, 224–235.

(40) Guénin, E.; Hervé, A.-C.; Floch, V.; Loisel, S.; Yaouanc, J.-J.; Clément, J.-C.; Férec, C.; des Abbayes, H. Cationic Phosphonolipids Containing Quaternary Phosphonium and Arsonium Groups for DNA Transfection with Good Efficiency and Low Cellular Toxicity**. *Angew. Chem. Int. Ed.* **2000**, *39*, 629–631.

(41) Heyes, J. A.; Niculescu-Duvaz, D.; Cooper, R. G.; Springer, C. J. Synthesis of Novel Cationic Lipids: Effect of Structural Modification on the Efficiency of Gene Transfer. *J. Med. Chem.* **2002**, *45*, 99–114.

(42) Boussif, O.; Lezoualc'h, F.; Zanta, M. A.; Mergny, M. D.; Scherman, D.; Demeneix, B.; Behr, J. P. A Versatile Vector for Gene and Oligonucleotide Transfer into Cells in Culture and in Vivo: Polyethylenimine. *Proc. Natl. Acad. Sci.* **1995**, *92* , 7297–7301.

(43) Katav, T.; Liu, L.; Traitel, T.; Goldbart, R.; Wolfson, M.; Kost, J. Modified Pectin-Based Carrier for Gene Delivery: Cellular Barriers in Gene Delivery Course. *J. Control. Release* **2008**, *130*, 183–191.

(44) Xu, F.-J.; Li, H.; Li, J.; Zhang, Z.; Kang, E.-T.; Neoh, K.-G. Pentablock Copolymers of Poly(ethylene Glycol), poly((2-Dimethyl Amino)ethyl Methacrylate) and poly(2-Hydroxyethyl Methacrylate) from Consecutive Atom Transfer Radical Polymerizations for Non-Viral Gene Delivery. *Biomaterials* **2008**, *29*, 3023–3033.

(45) Ho, Y. P.; Chen, H. H.; Leong, K. W.; Wang, T. H. Evaluating the Intracellular Stability and Unpacking of DNA Nanocomplexes by Quantum Dots-FRET. *J. Control. Release* **2006**, *116*, 83–89.

(46) Tkachenko, A. G.; Xie, H.; Liu, Y.; Coleman, D.; Ryan, J.; Glomm, W. R.; Shipton, M. K.; Franzen, S.; Feldheim, D. L. Cellular Trajectories of Peptide-Modified Gold Particle Complexes: Comparison of Nuclear Localization Signals and Peptide Transduction Domains. *Bioconjug. Chem.* **2004**, *15*, 482–490.

(47) Pantarotto, D.; Singh, R.; McCarthy, D.; Erhardt, M.; Briand, J. P.; Prato, M.; Kostarelos, K.; Bianco, A. Functionalized Carbon Nanotubes for Plasmid DNA Gene Delivery. *Angew. Chem. Int. Ed.* **2004**, *43*, 5242–5246.

(48) Le Corre, D.; Bras, J.; Dufresne, A. Starch Nanoparticles: A Review. *Biomacromolecules* **2010**, *11*, 1139–1153.

(49) Ellis, R. P.; Cochrane, M. P.; Dale, M. F. B.; Duffus, C. M.; Lynn, A.; Morrison, I. M.; Prentice, R. D. M.; Swanston, J. S.; Tiller, S. A. Starch Production and Industrial Use. *J. Sci. Food Agric.* **1998**, *77*, 289–311.

(50) Miles, M. J.; Morris, V. J.; Orford, P. D.; Ring, S. G. The Roles of Amylose and Amylopectin in the Gelation and Retrogradation of Starch. *Carbohydr. Res.* **1985**, *135*, 271–281.

(51) Tester, R. F.; Karkalas, J.; Qi, X. Starch—composition, Fine Structure and Architecture. *J. Cereal Sci.* **2004**, *39*, 151–165.

(52) Shi, A. M.; Li, D.; Wang, L. J.; Li, B. Z.; Adhikari, B. Preparation of Starch-Based Nanoparticles through High-Pressure Homogenization and Miniemulsion Cross-Linking: Influence of Various Process Parameters on Particle Size and Stability. *Carbohydr. Polym.* **2011**, *83*, 1604–1610.

(53) Uslu, M. K.; Polat, S. Effects of Glyoxal Cross-Linking on Baked Starch Foam. *Carbohydr. Polym.* **2012**, *87*, 1994–1999.

(54) Kim, H. S.; Hwang, D. K.; Kim, B. Y.; Baik, M. Y. Cross-Linking of Corn Starch with Phosphorus Oxychloride under Ultra High Pressure. *Food Chem.* **2012**, *130*, 977–980.

(55) O'Brien, S.; Wang, Y. J. Effects of Shear and pH on Starch Phosphates Prepared by Reactive Extrusion as a Sustained Release Agent. *Carbohydr. Polym.* **2009**, *77*, 464–471.

(56) Li, Y.; De Vries, R.; Slaghek, T.; Timmermans, J.; Cohen Stuart, M. A.; Norde, W. Preparation and Characterization of Oxidized Starch Polymer Microgels for Encapsulation and Controlled Release of Functional Ingredients. *Biomacromolecules* **2009**, *10*, 1931–1938.

(57) Li, Y.; Kadam, S.; Abee, T.; Slaghek, T. M.; Timmermans, J. W.; Cohen Stuart, M. A.; Norde, W.; Kleijn, M. J. Antimicrobial Lysozyme-Containing Starch Microgel to Target and Inhibit Amylase-Producing Microorganisms. *Food Hydrocoll.* **2012**, *28*, 28–35.

(58) Simi, C. K.; Emilia Abraham, T. Hydrophobic Grafted and Cross-Linked Starch Nanoparticles for Drug Delivery. *Bioprocess Biosyst. Eng.* **2007**, *30*, 173–180.

(59) Šimkovic, I.; Hricovíni, M.; Mendichi, R.; Van Soest, J. J. G. Cross-Linking of Starch with 1, 2, 3, 4-Diepoxybutane or 1, 2, 7, 8-Diepoxyoctane. *Carbohydr. Polym.* **2004**, *55*, 299–305.

(60) Bajpai, A. K.; Bhanu, S. Dynamics of Controlled Release of Heparin from Swellable Crosslinked Starch Microspheres. *J. Mater. Sci. Mater. Med.* **2007**, *18*, 1613–1621.

(61) Hamdi, G.; Ponchel, G. Enzymatic Degradation of Epichlorohydrin Crosslinked Starch Microspheres by Alpha-Amylase. *Pharm. Res.* **1999**, *16*, 867–875.

(62) Likhitkar, S.; Bajpai, A. K. Magnetically Controlled Release of Cisplatin from Superparamagnetic Starch Nanoparticles. *Carbohydr. Polym.* **2012**, *87*, 300–308.

(63) Ma, X.; Jian, R.; Chang, P. R.; Yu, J. Fabrication and Characterization of Citric Acid-Modified Starch Nanoparticles/plasticized-Starch Composites. *Biomacromolecules* **2008**, *9*, 3314–3320.

(64) Reddy, N.; Yang, Y. Citric Acid Cross-Linking of Starch Films. *Food Chem.* **2010**, *118*, 702–711.

(65) Kumar, A. P.; Singh, R. P. Biocomposites of Cellulose Reinforced Starch: Improvement of Properties by Photo-Induced Crosslinking. *Bioresour. Technol.* **2008**, *99*, 8803–8809.

(66) Wattanachant, S.; Muhammad, K.; Mat Hashim, D.; Rahman, R. A. Effect of Crosslinking Reagents and Hydroxypropylation Levels on Dual-Modified Sago Starch Properties. *Food Chem.* **2003**, *80*, 463–471.

(67) Yu, D.; Xiao, S.; Tong, C.; Chen, L.; Liu, X. Dialdehyde Starch Nanoparticles: Preparation and Application in Drug Carrier. *Chin. Sci. Bull.* **2007**, *52*, 2913–2918.

(68) Hedin, J.; Östlund, Å.; Nydén, M. UV Induced Cross-Linking of Starch Modified with Glycidyl Methacrylate. *Carbohydr. Polym.* **2010**, *79*, 606–613.

(69) Moad, G. Chemical Modification of Starch by Reactive Extrusion. *Prog. Polym. Sci.* **2011**, *36*, 218–237.

(70) Xie, F.; Yu, L.; Liu, H.; Chen, L. Starch Modification Using Reactive Extrusion. *Starch - Stärke* **2006**, *58*, 131–139.

(71) Seker, M.; Hanna, M. A. Cross-Linking Starch at Various Moisture Contents by Phosphate Substitution in an Extruder. *Carbohydr. Polym.* **2005**, *59*, 541–544.

(72) Wildi, R. H.; Van Egdob, E.; Bloembergen, S. Process for Producing Biopolymer Nanoparticles. US20110042841 A1, 2011.

(73) Bloemberger, S.; Lee, D. I.; Mclennan, I. J.; Wildi, R. H.; Van, E. E. Process for Producing Biopolymer Nanoparticle Biolatex Compositions Having Enhanced Performance and Compositions Based Thereon. CA2745303 A1, 2010.

(74) Wang, G.; Thompson, M. R.; Liu, Q. Controlling the Moisture Absorption Capacity in a Fiber-Reinforced Thermoplastic Starch Using Sodium Trimetaphosphate. *Ind. Crops Prod.* **2012**, *36*, 299–303.

(75) Cioica, N.; Fechete, R.; Cota, C.; Nagy, E. M.; David, L.; Cozar, O. NMR Relaxation Investigation of the Native Corn Starch Structure with Plasticizers. *J. Mol. Struct.* **2013**, *1044*, 128–133.

(76) Li, D. M. H. Characterization, Quantification and Modification of Starch Nanoparticles, University of Waterloo, 2014.

(77) Bloembergen, S. Methods of Using Biobased Latex Binders for Improved Printing Performance. WO/2011/084692, 2011.

(78) Chakraborty, S.; Sahoo, B.; Teraoka, I.; Miller, L. M.; Gross, R. A. Enzyme-Catalyzed Regioselective Modification of Starch Nanoparticles. *Macromolecules* **2005**, *38*, 61–68.

(79) Chakraborty, S.; Sahoo, B.; Teraoka, I.; Gross, R. A. Solution Properties of Starch Nanoparticles in Water and DMSO as Studied by Dynamic Light Scattering. *Carbohydr. Polym.* **2005**, *60*, 475–481.

(80) Rodrigues, A.; Emeje, M. Recent Applications of Starch Derivatives in Nanodrug Delivery. *Carbohydr. Polym.* **2012**, *87*, 987–994.

(81) Santander-Ortega, M. J.; Stauner, T.; Loretz, B.; Ortega-Vinuesa, J. L.; Bastos-González, D.; Wenz, G.; Schaefer, U. F.; Lehr, C. M. Nanoparticles Made from Novel Starch Derivatives for Transdermal Drug Delivery. *J. Control. Release* **2010**, *141*, 85–92.

(82) Kato, Y.; Matsuo, R.; Isogai, A. Oxidation Process of Water-Soluble Starch in TEMPO-Mediated System. *Carbohydr. Polym.* **2003**, *51*, 69–75.

(83) Fraschini, C.; Vignon, M. R. Selective Oxidation of Primary Alcohol Groups of Beta-Cyclodextrin Mediated by 2,2,6,6-Tetramethylpiperidine-1-Oxyl Radical (TEMPO). *Carbohydr. Res.* **2000**, *328*, 585–589.

(84) Chan, H. T.; Bhat, R.; Karim, A. A. Physicochemical and Functional Properties of Ozone-Oxidized Starch. *J. Agric. Food Chem.* **2009**, *57*, 5965–5970.

(85) An, H. J.; King, J. M. Using Ozonation and Amino Acids to Change Pasting Properties of Rice Starch. *J. Food Sci.* **2009**, *74*.

(86) Klein, B.; Vanier, N. L.; Moomand, K.; Pinto, V. Z.; Colussi, R.; Da Rosa Zavareze, E.; Dias, A. R. G. Ozone Oxidation of Cassava Starch in Aqueous Solution at Different pH. *Food Chem.* **2014**, *155*, 167–173.

(87) Lawal, O. S.; Lechner, M. D.; Hartmann, B.; Kulicke, W. M. Carboxymethyl Cocoyam Starch: Synthesis, Characterisation and Influence of Reaction Parameters. *Starch/Staerke* **2007**, *59*, 224–233.

(88) Liu, J.; Ming, J.; Li, W.; Zhao, G. Synthesis, Characterisation and in Vitro Digestibility of Carboxymethyl Potato Starch Rapidly Prepared with Microwave-Assistance. *Food Chem.* **2012**, *133*, 1196–1205.

(89) Wang, L. F.; Pan, S. Y.; Hu, H.; Miao, W. H.; Xu, X. Y. Synthesis and Properties of Carboxymethyl Kudzu Root Starch. *Carbohydr. Polym.* **2010**, *80*, 174–179.

(90) Granö, H.; Yli-Kauhaluoma, J.; Suortti, T.; Käki, J.; Nurmi, K. Preparation of Starch Betainate: A Novel Cationic Starch Derivative. *Carbohydr. Polym.* **2000**, *41*, 277–283.

(91) Pal, S.; Mal, D.; Singh, R. P. Cationic Starch: An Effective Flocculating Agent. *Carbohydr. Polym.* **2005**, *59*, 417–423.

(92) Wang, Y.; Xie, W. Synthesis of Cationic Starch with a High Degree of Substitution in an Ionic Liquid. *Carbohydr. Polym.* **2010**, *80*, 1172–1177.

(93) Wei, Y.; Cheng, F.; Zheng, H. Synthesis and Flocculating Properties of Cationic Starch Derivatives. *Carbohydr. Polym.* **2008**, *74*, 673–679.

(94) Amar-Lewis, E.; Azagury, A.; Chintakunta, R.; Goldbart, R.; Traitel, T.; Prestwood, J.; Landesman-Milo, D.; Peer, D.; Kost, J. Quaternized Starch-Based Carrier for siRNA Delivery: From Cellular Uptake to Gene Silencing. *J. Control. Release* **2014**, *185*, 109–120.

(95) Bohrisch, J.; Vorwerg, W.; Radosta, S. Development of Hydrophobic Starch. *Starch/Staerke* **2004**, *56*, 322–329.

(96) Namazi, H.; Fathi, F.; Dadkhah, A. Hydrophobically Modified Starch Using Long-Chain Fatty Acids for Preparation of Nanosized Starch Particles. *Sci. Iran.* **2011**, *18*, 439–445.

(97) Ou, S.; Yang, A. L. A. A Study on Synthesis of Starch Ferulate and Its Biological Properties. *Food Chem.* **2001**, *74*, 91–95.

(98) Dandekar, P.; Jain, R.; Stauner, T.; Loretz, B.; Koch, M.; Wenz, G.; Lehr, C. M. A Hydrophobic Starch Polymer for Nanoparticle-Mediated Delivery of Docetaxel. *Macromol. Biosci.* **2012**, *12*, 184–194.

(99) Chang, P. R.; Ai, F.; Chen, Y.; Dufresne, A.; Huang, J. Effects of Starch Nanocrystal-Graft-Porycaprolactone on Mechanical Properties of Waterborne Polyurethane-Based Nanocomposites. *J. Appl. Polym. Sci.* **2009**, *111*, 619–627.

(100) Xu, Y.; Ding, W.; Liu, J.; Li, Y.; Kennedy, J. F.; Gu, Q.; Shao, S. Preparation and Characterization of Organic-Soluble Acetylated Starch Nanocrystals. *Carbohydr. Polym.* **2010**, *80*, 1078–1084.

(101) Qiao, L.; Gu, Q. M.; Cheng, H. N. Enzyme-Catalyzed Synthesis of Hydrophobically Modified Starch. *Carbohydr. Polym.* **2006**, *66*, 135–140.

(102) Garg, S.; Jana, A. K. Characterization and Evaluation of Acylated Starch with Different Acyl Groups and Degrees of Substitution. *Carbohydr. Polym.* **2011**, *83*, 1623–1630.

(103) Ohya, Y.; Masunaga, T.; Baba, T.; Ouchi, T. Synthesis and Cytotoxic Activity of Dextran-Immobilizing Platinum(II) Complex Through Chelate-Type Coordination Bond. *J. Macromol. Sci. Part A* **1996**, *33*, 1005–1016.

(104) Kovács, A. F.; Turowski, B. Chemoembolization of Oral and Oropharyngeal Cancer Using a High-Dose Cisplatin Crystal Suspension and Degradable Starch Microspheres. *Oral Oncol.* **2002**, *38*, 87–95.

(105) Xiao, S.; Tong, C.; Liu, X.; Yu, D.; Liu, Q.; Xue, C.; Tang, D.; Zhao, L. Preparation of Folate-Conjugated Starch Nanoparticles and Its Application to Tumor-Targeted Drug Delivery Vector. *Chinese Sci. Bull.* **2006**, *51*, 1693–1697.

(106) Shalviri, A.; Chan, H. K.; Raval, G.; Abdekhodaie, M. J.; Liu, Q.; Heerklotz, H.; Wu, X. Y. Design of pH-Responsive Nanoparticles of Terpolymer of Poly(methacrylic Acid), Polysorbate 80 and Starch for Delivery of Doxorubicin. *Colloids Surf. B. Biointerfaces* **2013**, *101*, 405–413.

(107) Yamada, H.; Loretz, B.; Lehr, C.-M. M. Design of Starch-Graft-PEI Polymers: An Effective and Biodegradable Gene Delivery Platform. *Biomacromolecules* **2014**, *15*, 1753–1761.

(108) Zhu, Y.; Wu, Z.; Tang, Z.; Lu, Z. HeLa Cell Adhesion on Various Collagen-Grafted Surfaces. *J. Proteome Res.* **2002**, *1*, 559–562.

(109) Nelson-Rees, W. A.; Flandermeyer, R. R. HeLa Cultures Defined. *Science* **1976**, *191*, 96–98.

(110) Ferrari, M.; Fornasiero, M. C.; Isetta, A. M. MTT Colorimetric Assay for Testing Macrophage Cytotoxic Activity in Vitro. *J. Immunol. Methods* **1990**, *131*, 165–172.

(111) Gerlier, D.; Thomasset, N. Use of MTT Colorimetric Assay to Measure Cell Activation. *J. Immunol. Methods* **1986**, *94*, 57–63.

(112) Van Meerloo, J.; Kaspers, G. J. L.; Cloos, J. Cell Sensitivity Assays: The MTT Assay. *Methods Mol. Biol.* **2011**, *731*, 237–245.

(113) American Type Culture Collection. MTT Cell Proliferation Assay Instruction Guide. *Components* **2011**, *6597*, 1–6.

(114) Shangari, N.; O'Brien, P. J. The Cytotoxic Mechanism of Glyoxal Involves Oxidative Stress. *Biochem. Pharmacol.* **2004**, *68*, 1433–1442.

(115) Kasper, M.; Roehlecke, C.; Witt, M.; Fehrenbach, H.; Hofer, A.; Miyata, T.; Weigert, C.; Funk, R. H. W.; Schleicher, E. D. Induction of Apoptosis by Glyoxal in Human Embryonic Lung Epithelial Cell Line L132. *Am. J. Respir. Cell Mol. Biol.* **2000**, *23*, 485–491.

(116) Reber, F.; Kasper, M.; Siegner, A.; Kniep, E.; Seigel, G.; Funk, R. H. W. Alteration of the Intracellular pH and Apoptosis Induction in a Retinal Cell Line by the AGE-Inducing Agent Glyoxal. *Graefes Arch. Clin. Exp. Ophthalmol.* **2002**, *240*, 1022–1032.

(117) De Nooy, A. E. J.; Besemer, A. C.; Van Bekkum, H. Selective Oxidation of Primary Alcohols Mediated by Nitroxyl Radical in Aqueous Solution. Kinetics and Mechanism. *Tetrahedron* **1995**, *51*, 8023–8032.

(118) Ip, A. C.-F.; Tsai, T. H.; Khimji, I.; Huang, P.-J. J.; Liu, J. Degradable Starch Nanoparticle Assisted Ethanol Precipitation of DNA. *Carbohydr. Polym.* **2014**, *110*, 354–359.

(119) Carvalho, C.; Santos, R. X.; Cardoso, S.; Correia, S.; Oliveira, P. J.; Santos, M. S.; Moreira, P. I. Doxorubicin: The Good, the Bad and the Ugly Effect. *Curr. Med. Chem.* **2009**, *16*, 3267–3285.

(120) Allen, T. M.; Cullis, P. R. Drug Delivery Systems: Entering the Mainstream. *Science* **2004**, *303*, 1818–1822.

(121) Northfelt, D. W.; Martin, F. J.; Working, P.; Volberding, P. A.; Russell, J.; Newman, M.; Amantea, M. A.; Kaplan, L. D. Doxorubicin Encapsulated in Liposomes Containing Surface-Bound Polyethylene Glycol: Pharmacokinetics, Tumor Localization, and Safety in Patients with AIDS-Related Kaposi's Sarcoma. *J. Clin. Pharmacol.* **1996**, *36*, 55–63.

(122) Elbayoumi, T. A.; Torchilin, V. P. Tumor-Specific Anti-Nucleosome Antibody Improves Therapeutic Efficacy of Doxorubicin-Loaded Long-Circulating Liposomes against Primary and Metastatic Tumor in Mice. *Mol. Pharm.* **2009**, *6*, 246–254.

(123) Zhang, Z.; Chen, X.; Chen, L.; Yu, S.; Cao, Y.; He, C.; Chen, X. Intracellular pH-Sensitive PEG-Block-Acetalated-Dextrans as Efficient Drug Delivery Platforms. *ACS Appl. Mater. Interfaces* **2013**, *5*, 10760–10766.

(124) Yao, X.; Chen, L.; Chen, X.; He, C.; Zheng, H.; Chen, X. Intercellular pH-Responsive Histidine Modified Dextran-G-Cholesterol Micelle for Anticancer Drug Delivery. *Colloids Surf. B. Biointerfaces* **2014**, *121*, 36–43.

(125) Yoo, H. S.; Park, T. G. Folate-Receptor-Targeted Delivery of Doxorubicin Nano-Aggregates Stabilized by Doxorubicin-PEG-Folate Conjugate. *J. Control. Release* **2004**, *100*, 247–256.

(126) Yoo, H. S.; Park, T. G. Folate Receptor Targeted Biodegradable Polymeric Doxorubicin Micelles. *J. Control. Release* **2004**, *96*, 273–283.

(127) Lee, R. J.; Low, P. S. Folate-Mediated Tumor-Cell Targeting of Liposome-Entrapped Doxorubicin in-Vitro. *Biochim. Biophys. Acta-Biomembranes* **1995**, *1233*, 134–144.

(128) Bachelder, E. M.; Beaudette, T. T.; Broaders, K. E.; Dashe, J.; Fréchet, J. M. J. Acetal-Derivatized Dextran: An Acid-Responsive Biodegradable Material for Therapeutic Applications. *J. Am. Chem. Soc.* **2008**, *130*, 10494–10495.

(129) Bae, Y.; Fukushima, S.; Harada, A.; Kataoka, K. Design of Environment-Sensitive Supramolecular Assemblies for Intracellular Drug Delivery: Polymeric Micelles That Are Responsive to Intracellular pH Change. *Angew. Chem. Int. Ed.* **2003**, *42*, 4640–4643.

(130) Mitra, S.; Gaur, U.; Ghosh, P. C.; Maitra, A. N. Tumour Targeted Delivery of Encapsulated Dextran-Doxorubicin Conjugate Using Chitosan Nanoparticles as Carrier. *J. Control. Release* **2001**, *74*, 317–323.

(131) Li, M.; Tang, Z.; Lv, S.; Song, W.; Hong, H.; Jing, X.; Zhang, Y.; Chen, X. Cisplatin Crosslinked pH-Sensitive Nanoparticles for Efficient Delivery of Doxorubicin. *Biomaterials* **2014**, *35*, 3851–3864.

(132) Schanen, B. C.; Karakoti, A. S.; Seal, S.; Drake, D. R.; Warren, W. L.; Self, W. T. Exposure to Titanium Dioxide Nanomaterials Provokes Inflammation of an in Vitro Human Immune Construct. *ACS Nano* **2009**, *3*, 2523–2532.